Steamed broccoli sprouts alleviate gut inflammation and retain gut microbiota against DSS-induced symptoms.

Johanna M. Holman[1], Louisa Colucci[2], Dorien Baudewyns[3], Joe Balkan[4], Timothy Hunt[5], Benjamin Hunt[5], Lola Holcomb[6], Grace Chen[7], Peter L. Moses[8,9], Gary M. Mawe[8], Tao Zhang[10], Yanyan Li[1*], Suzanne L. Ishaq[1*]

[1] School of Food and Agriculture, University of Maine, Orono, Maine, USA 04469
[2] Department of Biology, Husson University, Bangor, Maine, USA 04401
[3] Department of Psychology, University of Maine, Orono, USA 04469
[4] Department of Chemical and Biological Engineering, Tufts University, Medford, Massachusetts, USA 02155
[5] Department of Biology, University of Maine, Orono, Maine, USA 04469
[6] Graduate School of Biomedical Sciences and Engineering, University of Maine, Orono, Maine, USA 04469
[7] Department of Internal Medicine, University of Michigan Medical School, Ann Arbor, Michigan, USA 48109
[8] Departments of Neurological Sciences and of Medicine, Larner College of Medicine, University of Vermont, Burlington, Vermont, USA 05401
[9] Finch Therapeutics, Somerville, Massachusetts, USA 02143
[10] School of Pharmacy and Pharmaceutical Sciences, SUNY Binghamton University, Johnson City, New York, USA 13790

***Corresponding authors:**
Suzanne L. Ishaq, University of Maine, School of Food and Agriculture, Orono, ME 04469, sue.ishaq@maine.edu, 1-207-581-2770
Yanyan Li, University of Maine, School of Food and Agriculture, Orono, ME 04469, yanyan.li@maine.edu, 1-207-581-3134

Keywords: inflammatory bowel disease, ulcerative colitis, broccoli, broccoli sprouts, sulforaphane, glucoraphanin, gut microbiota, dietary bioactives.

Abstract: Inflammatory Bowel Diseases (IBD) are devastating conditions of the gastrointestinal tract with limited treatments, and dietary intervention may be effective, affordable, and safe for managing symptoms. Ongoing research has identified inactive compounds in broccoli sprouts, like glucoraphanin, and that mammalian gut microbiota play a role in metabolizing it to the anti-inflammatory sulforaphane. The biogeographic location of participating microbiota and how that affects anti-inflammatory benefits to the host is unknown. We fed specific pathogen free C57BL/6 mice either a control diet or a 10% steamed broccoli sprout diet, and gave a three-cycle regimen of 2.5% dextran sodium sulfate (DSS) in drinking water over a 34-day experiment to simulate chronic, relapsing ulcerative colitis. We monitored body weight, fecal characteristics, lipocalin, and bacterial communities from the contents and mucosa in the jejunum, cecum, and colon. Mice fed the broccoli sprout diet while receiving DSS performed better than mice fed the control diet while receiving DSS for all disease parameters, including significantly more weight gain, lower Disease Activity Index scores, lower serum lipocalin, and higher bacterial richness in all gut locations. Bacterial communities were assorted by gut location except in the mice receiving the control diet and DSS treatment. Importantly, our results suggested that broccoli sprout feeding effectively abrogated the effects of DSS on gut microbiota, as bacterial communities were similar between mice receiving broccoli sprouts with and without DSS. Collectively, these results strongly support the protective effect of steamed broccoli sprouts against gut microbiota dysbiosis and development of colitis induced by DSS.

Importance: Spatially resolved microbial communities provide greater insight than fecal microbial communities when investigating host-microbe interactions. Here, we show that a 10% broccoli sprout diet protects mice from the negative effects of dextran sodium sulfate induced

colitis, that colitis erases biogeographical patterns of bacterial communities in the gut, and that the cecum is not likely to be a significant contributor to colonic bacteria of interest in the DSS mouse model of ulcerative colitis. Mice fed the broccoli sprout diet while receiving DSS performed better than mice fed the control diet while receiving DSS for all disease parameters, including significantly more weight gain, lower Disease Activity Index scores. Broccoli sprouts represent an affordable, accessible, and safe method of resolving DSS-induced inflammation and colitis. Information on how the gut microbiome mediates health benefits is critical to making effective medical recommendations.

Introduction

Inflammatory Bowel Diseases (IBD) are globally prevalent, chronic inflammatory diseases of multifactorial origin with an annual healthcare cost of billions of dollars in the United States alone (1, 2). IBD occurs in the gastrointestinal tract, and can be accompanied by autoimmune dysfunction, leading to microbial community changes in the gut. In addition to being chronic and debilitating, a longer duration of IBD is associated with an increased risk of developing gastrointestinal cancers such as colorectal cancer (3–6). Treatments are currently limited to alleviating inflammatory symptoms, and returning patients to as close to homeostasis as possible. Diet can play an important role in the management of IBD as a source of anti-inflammatory metabolites, and as a tool for influencing the robustness of gut microbiomes. However, many guidelines for IBD patients recommend avoiding sulfur-rich foods which produce metabolites that might exacerbate symptoms in the gut (7), even as other sulfurous components reduce symptoms (8). Diet can be beneficial or detrimental to gut inflammation (9), but IBD patients choose to avoid all fiber based on a lost nuance that only some fiber sources and situations may induce negative

81 side effects, e.g., (10). Thus, a better understanding of the interaction of diet, microorganisms, and
82 disease is needed before dietary recommendations can be made.

83 Diets which are high in cruciferous vegetables such as broccoli have been associated with
84 reduced inflammation and cancer risk (11–15) due to a group of specific plant secondary
85 compounds, glucosinolates, which are used for defense against insect herbivory. Glucosinolates
86 are very high in broccoli and can be converted into bioactive metabolites (16–18) such as sulfur-
87 containing isothiocyanates, by the action of myrosinase, an enzyme present in these vegetables. In
88 humans, isothiocyanates have been identified as bioactive candidates for reducing gut
89 inflammation (19–21). Specifically, sulforaphane (SFN), a well-studied isothiocyanate (22), has
90 been shown to inhibit the action of Nuclear Factor – Kappa B (NF-κB) and Signal Transducer and
91 Activator Of Transcription 3 (STAT3) which are responsible for upregulation of inflammatory
92 cytokines interleukins-6, -8, -12, -21, and -23 (19, 23–26). However, raw broccoli and broccoli
93 sprouts contain small amounts of this anti-inflammatory, as broccoli-sourced enzymes
94 preferentially metabolize the precursor of sulforaphane, glucoraphanin (GLR), to an inactive
95 byproduct instead (22). Cooking the sprouts can alter the enzymatic activity of broccoli enzymes
96 to prevent the creation of an inactive byproduct, leaving glucosinolates intact.

97 Mammals do not produce the enzymes for converting glucosinolates to isothiocyanates;
98 however, gut bacteria with β-thioglucosidase activity can convert GLR to bioactive SFN in the
99 mammalian GI tract (27–29). In human participants who were pretreated with oral antibiotics and
100 bowel cleansing, urinary isothiocyanates excretion after consumption of cooked broccoli
101 decreased significantly (17), supporting a role for gut microbiota. Several microorganisms isolated
102 from the mammalian gut appear to have myrosinase-like enzymes that cleave the glycoside moiety
103 from glucosinolates precursors, and there is evidence for GLR hydrolysis to SFN by colonic and

104 cecal bacteria, *ex vivo* and *in vivo* in mono-colonized animal models (27, 30, 31). The bacterial
105 populations that are capable of metabolizing glucosinolates precursors are not fully known, but
106 *Lactobacillus*, *Bifidobacteria,* and *Bacteroides* strains have been implicated (20, 31, 32).

107 The taxonomic and functional structure of microbial communities along the
108 gastrointestinal tract are highly dependent on the diet, health status, age, and microbial encounters
109 of the host (33–35). Specific organs and sites within organs foster different environmental
110 conditions that can create spatial niches for microbial taxa, an ecological pattern known as
111 biogeography (36–38). For example, pH changes dramatically along the gastrointestinal tract and
112 is linked to microbial diversity and density. IBD patients often have a less acidic gastrointestinal
113 tract (39) due to altered diet or treatments, and this may result in alterations to gut biogeography
114 (40), especially in mucosal-associated bacterial fractions (41–43). Mouse studies suggest
115 biotransformation of GLR to SFN occurs in the colon (31, 44, 45), and we confirmed the majority
116 of SFN accumulation to occur in the colon with greater resolution using multiple locations along
117 the GI tract in our recently published study (18). Altering the structure and function of bacterial
118 communities could alter if and where sulforaphane is created, which would improve or lessen the
119 impact of having a locally produced anti-inflammatory on the destructive effects of colitis.

120 The dextran sodium sulfate (DSS) mouse model is widely used to reflect human Ulcerative
121 Colitis (UC) in many ways (46, 47), and has been used for studying diet-sourced anti-
122 inflammatories for the prevention of IBD in animals (46, 48). Administration of DSS in drinking
123 water modifies the expression of tight junction proteins in intestinal epithelial cells, leading to a
124 leaky epithelial barrier (49). This is followed by goblet cell depletion, erosion, ulceration, and
125 infiltration of neutrophils into the lamina propria and submucosa (50), triggering the innate
126 immune response (51, 52).

127 There are significant knowledge gaps regarding the biogeography of the participating
128 microbiota and how this may impact glucosinolate metabolism and health benefits to the host; and
129 meanwhile, how the populations of microbiota are impacted by these bioactives remains unclear.
130 To address these, we assessed the impact of steamed broccoli sprouts on the biogeographic pattern
131 of gut microbiota and disease outcome in a mouse model of chronic, relapsing colitis. We fed
132 specific pathogen free (SPF) C57BL/6 mice either a control diet or a 10% steamed broccoli sprout
133 diet, starting at 6 weeks of age and continuing for another 40 days. The fresh broccoli sprouts were
134 steamed to inactivate plant enzymes, and thus the metabolism of glucosinolates to isothiocyanates
135 would rely on the gut microbiota. A three-cycle regimen of DSS in drinking water was given to
136 stimulate chronic colitis in the mice, which is a well-established method (48, 53). We analyzed the
137 bacterial communities from the luminal-associated (i.e., digesta contents) and mucosal-associated
138 (i.e., scrapings) fractions in the jejunum, cecum, and colon using 16S rRNA gene sequencing, and
139 compared this to metrics of disease activity including weight gain/stagnation, fecal characteristics,
140 and lipocalin as a surrogate marker for inflammation in IBD (Figure 1).
141
142
143 **Results**
144 **Broccoli sprouts alleviated disease characteristics of DSS-induced colitis**
145 Mice were divided into four groups: control diet (Control), control diet with 2.5% DSS in
146 drinking water (Control+DSS), 10% (w/w) steamed broccoli sprout diet (Broccoli, with the control
147 diet as the base), and 10% broccoli sprout diet with 2.5% DSS in drinking water (Broccoli+DSS)
148 (Figure 1). The DSS regimen was designed to induce chronic, relapsing colitis (54). The 6-week-

old mice were acclimatized for 1 week. Treatment began in two phases: broccoli mice began their treatment at 7 weeks old (Day 0), and the first DSS cycle began at 8 weeks old (Day 8).

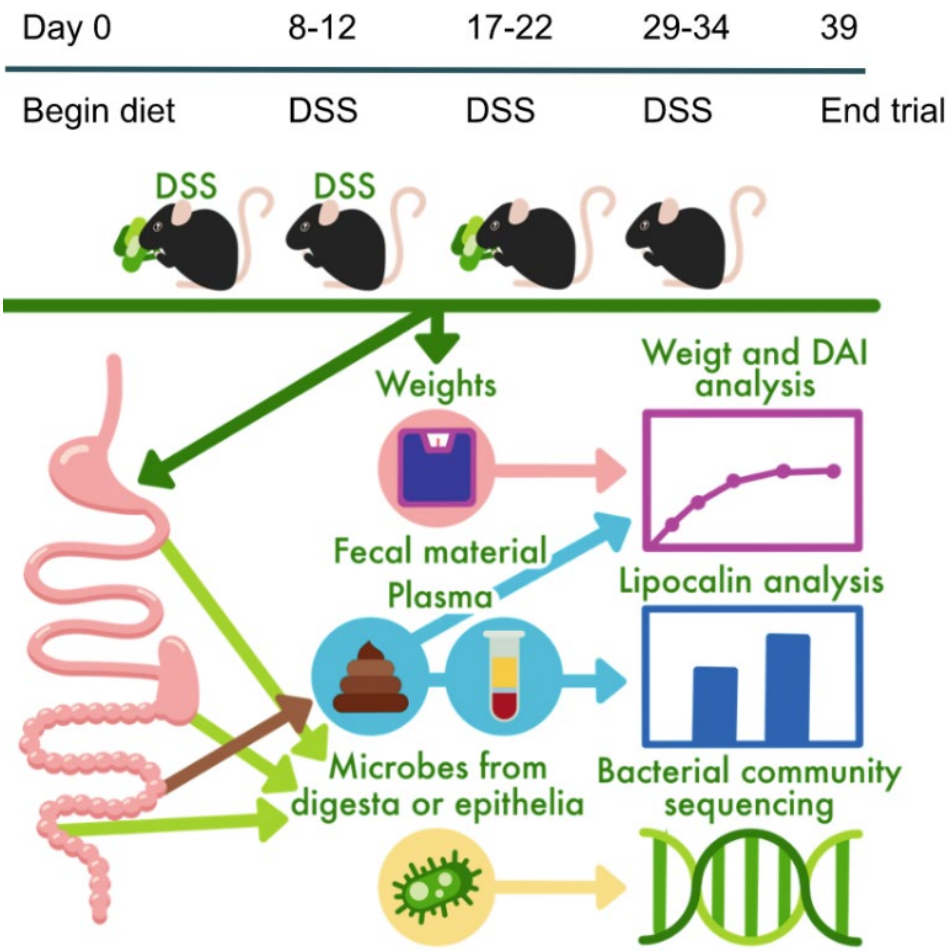

Figure 1. Experimental design schematic for a chronic model of colitis induced by dextran sodium sulfate (DSS) in 40 male mice (C57BL/6) beginning at 6-weeks of age.

All mice gained weight over the study, as they are in a growth phase at this age (55). Mice receiving the steamed broccoli sprout diet and DSS (Broccoli+DSS) gained significantly more body weight over the trial than mice given the control diet and DSS (Control+DSS) (Figure 2a; ANOVA, $p < 0.03$). There was no statistical difference observed in body weight among the three groups, Broccoli+DSS, Broccoli, and Control (ANOVA, $p > 0.05$). Control and Broccoli mice

occasionally exhibited slight weight loss as compared to body weight two days prior (Figure 2a), but these appeared to be random incidents which may be attributable to mice behavior and social dynamics. At the end of the first round of DSS treatment, Broccoli+DSS mice exhibited some weight loss and Control+DSS mice exhibited substantial weight loss (Figure 2a), but the second and third round of DSS only caused weight stagnation.

Mice in the Control+DSS group demonstrated elevated Disease Activity Index (DAI) scores as calculated by weight loss intensity score, fecal blood, and fecal consistency. Elevated DAI scores began at day 8 and lasted until day 34 (Figure 2b), and were significant on specific dates as compared to the mice in the Control group (Figure 2b, ANOVA, $p < 0.05$, comparisons by day, adjusted with TukeyHSD for multiple comparisons), as well as integrated over time (generalized additive model (GAM), $F = 308.32$, $p < 2e\text{-}16$).

Mice in the Broccoli+DSS group exhibited slightly elevated DAI scores during periods of DSS treatment, which returned to nearly 0 during rest periods, and which were lower as compared to Control+DSS mice (Figure 2b). Broccoli+DSS DAI scores were significantly elevated on specific dates (Figure 2b, ANOVA, $p < 0.05$, comparisons by treatment, adjusted with TukeyHSD for multiple comparisons), as well as integrated over time (GAM, $F = 17.47$, $p < 2e\text{-}16$). After the first round of DSS treatment, Broccoli+DSS and Control+DSS mice had similar elevated DAI scores (Figure 2b, ANOVA, $p > 0.05$). The diet control groups which were not treated with DSS, Control and Broccoli, did not have significantly different DAI scores from each other at any specific date (ANOVA, $p > 0.05$) or over time (GAM, $p > 0.05$). There was a lot of variability in the amount of fecal lipocalin between mice in treatment groups (Figure 3A), resulting in a lack of statistical significance between mice receiving DSS on the control diet and the steamed broccoli sprout diet except for day 19 on which steamed group had significantly (ANOVA, $p < 0.05$) higher

lipocalin levels. Analysis of plasma samples showed DSS increased lipocalin levels in the plasma (Figure 3B). Feeding the mice with a 10% broccoli sprouts diet reduced the lipocalin levels in the group of mice treated with DSS comparable to the control group without DSS treatment (ANOVA, $p < 0.05$).

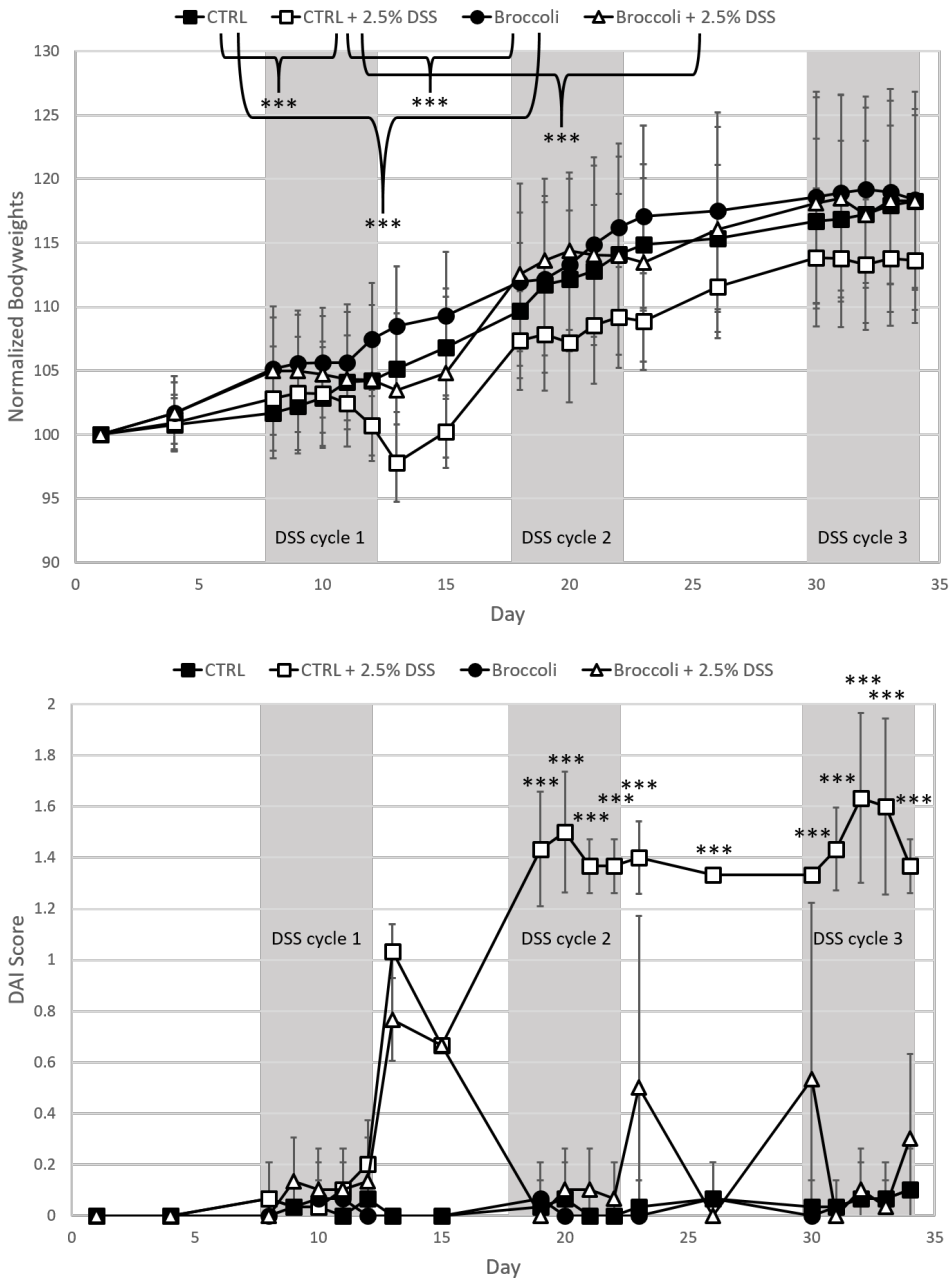

Figure 2. Metrics of disease status in a DSS-Induced model of chronic colitis, including (A) mouse body weights and (B) Disease Activity Index, by day of experiment. Body weights and

192 time scale were normalized to the day mice began the broccoli sprout diet. DAI scores are
193 calculated by weight loss intensity score, fecal blood, and fecal consistency. Treatment
194 comparisons at each day compared by ANOVA, and significance is designated as 0 - 0.001 '***'.
195 Four treatment groups were used in a 34-day chronic, relapsing model of colitis: control diet,
196 control diet with DSS added to drinking water, control diet adjusted with 10% by weight steamed
197 broccoli sprouts, and 10% broccoli sprout diet with DSS added to drinking water.

198

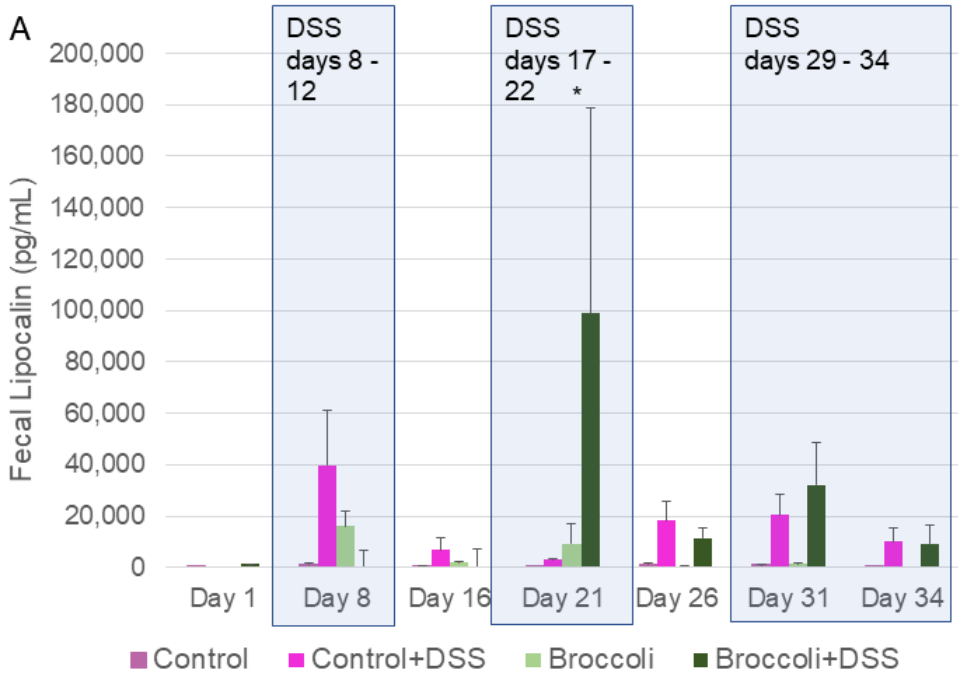

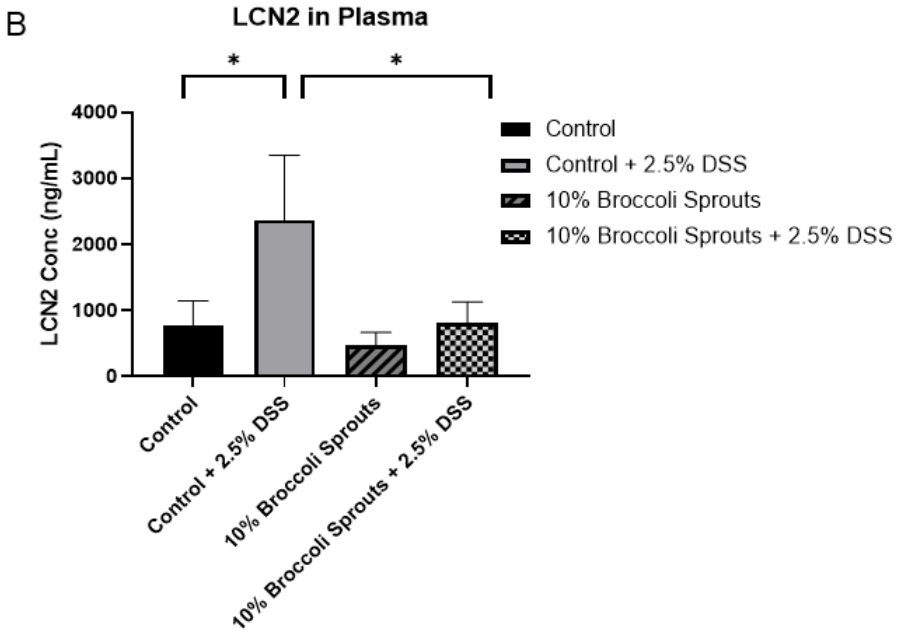

199

200 **Figure 3 Lipocalin in (A) feces at multiple timepoints and (B) serum on the last day of the**
201 **trial from mice in a DSS-Induced model of chronic colitis.** Significance was determined as $p <$
202 0.05, ANOVA.

203

204 Of the mice which had an elevated DAI score, some mice were positive for fecal blood,
205 which can select for certain bacteria in the gut. In a subset of samples of mice which had an
206 elevated DAI and were positive for fecal occult blood, there were different gut bacteria which were
207 identified as important community features depending on whether they received the Control+DSS
208 or the Broccoli+DSS diets (Figure 4, $p < 0.05$)). In Broccoli+DSS mice with positive fecal blood
209 scores, these important taxa included a bacterial sequence variant (SV) identified in the
210 Muribaculaceae family, and one in the *Clostridium* sensu stricto clade (Figure 4). For
211 Control+DSS mice with a positive fecal blood score, this included different SVs identified in the
212 *Clostridium* sensu stricto clade, *Cutibacterium*, and others (Figure 4).

Figure 4. Gut bacterial taxa identified from mice receiving DSS which were associated with having a positive fecal occult blood score on the last day of the experiment, by treatment. Data were subset to mice with a positive score on the last day of the experiment, when the gut samples were collected. Important features (SVs) were identified through permutational random forest analysis, and only the features important to this group (>50 reads) are listed out of 143 significant ($p < 0.05$) features across all treatments. Model accuracy was 89.7%. Bacterial sequence variants (SV) are identified as the lowest level of taxonomic identity possible, with "NA" indicating which could not be identified to species, and the number indicating which specific SV it was. Four treatment groups were used in a 34-day chronic, relapsing model of colitis, those included here are a control diet with DSS added to drinking water, and 10% broccoli sprout diet with DSS added to drinking water.

225

226 **Broccoli sprouts increased bacterial richness even during colitis**

227 Across all treatments and all mouse gastrointestinal samples, bacteria were primarily
228 identified as belonging to the phyla Bacillota (formerly Firmicutes), Bacteroidota (formerly
229 Bacteroidetes), Pseudomonadota (formerly Proteobacteria), Actinomycetota (formerly
230 Actinobacteria) which was higher in Control+DSS mice, and Verrucomicrobiota (formerly
231 Verrucomicrobia) which was higher in mice consuming broccoli sprouts (Figure S1).

232 Compared to the Control mice (receiving the control diet without DSS treatment), all other
233 treatment groups had more bacterial taxa present (measured as observed richness) in all locations
234 examined, with the exception of a loss of richness in the digesta/contents of the cecum and colon
235 in Control+DSS mice (Figure 5, Table 1, linear regression). Broccoli and Broccoli+DSS mice had
236 the highest bacterial richness in all gut locations, particularly in the colon contents and scraping,
237 but even the Control+DSS mice maintained high bacterial richness.

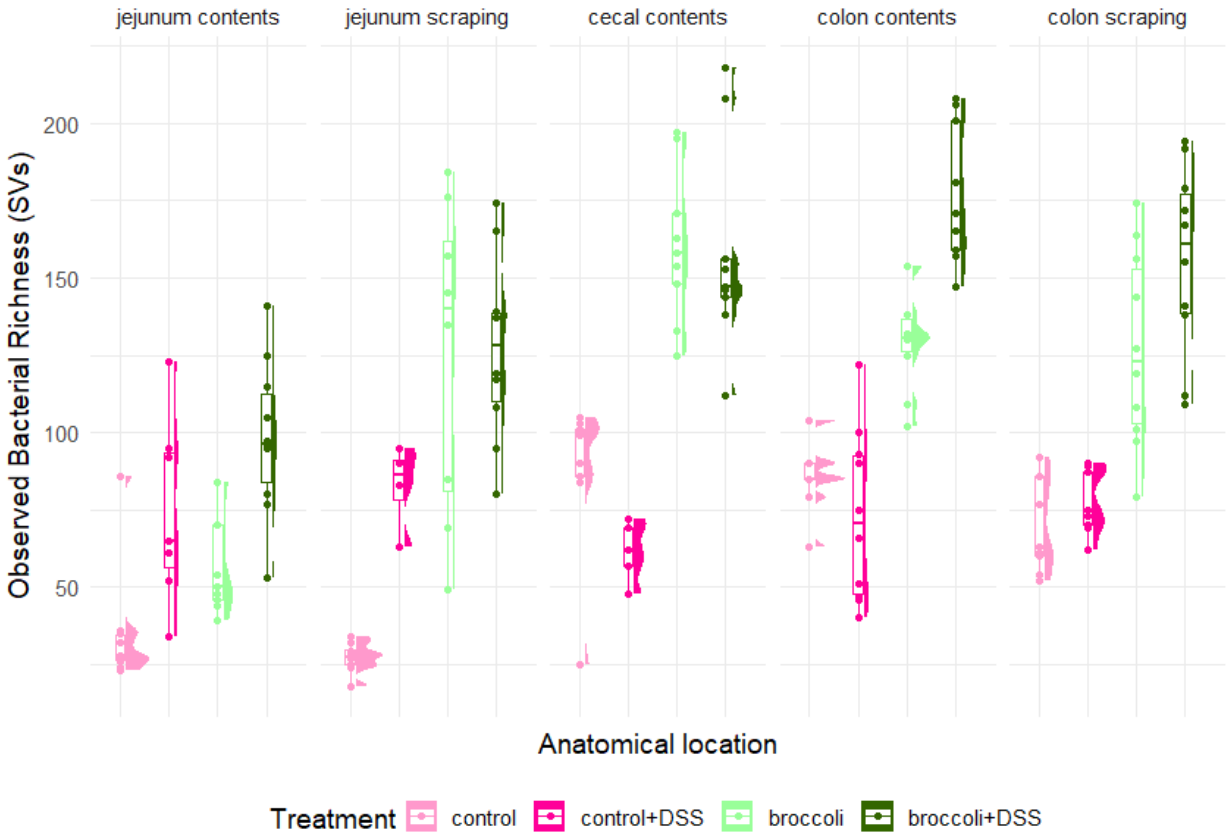

Figure 5. Observed bacterial richness along the intestinal of mice on control diets with or without broccoli sprouts, and with or without DSS-induced chronic repeating colitis. Richness is calculated as the number of different bacterial sequence variants (SVs). Statistically significant comparisons are provided in Table 1. Four treatment groups were used in a 34-day chronic, relapsing model of colitis: control diet, control diet with DSS added to drinking water, control diet adjusted with 10% by weight steamed broccoli sprouts, and 10% broccoli sprout diet with DSS added to drinking water.

Table 1. Statistical comparison of observed richness along the intestinal of mice on control diets with or without broccoli sprouts, and with or without DSS-induced chronic repeating colitis. Comparisons were made using linear regression models comparing treatment, in subsets of the data by anatomical location. Only significant comparisons ($p < 0.05$) are listed. Bacterial richness is visualized in Figure 5.

Treatment compared to control diet only group	Change in bacterial richness (SVs) ± Standard Error (rounded)	T-value	P-value

Jejunum contents			
Control + 2.5% DSS	40 ± 11	3.790	0.000608 ***
10% Broccoli sprouts	23 ± 10	2.766	0.009207 **
10% Broccoli sprouts + 2.5% DSS	64 ± 10	6.141	5.05e-07 ***
Jejunum scraping			
Control + 2.5% DSS	52 ± 17	3.`04	0.00434 **
10% Broccoli sprouts	98 ± 16	6.230	1.16e-06 ***
10% Broccoli sprouts + 2.5% DSS	100 ± 15	6.708	3.35e-07 ***
Cecum contents			
Control + 2.5% DSS	-13 ± 15	-0.821	0.418
10% Broccoli sprouts	68 ± 13	5.120	1.54e-05 ***
10% Broccoli sprouts + 2.5% DSS	70 ± 13	5.225	1.54e-05 ***
Colon contents			
Control + 2.5% DSS	-12 ± 9	-1.316	0.197
10% Broccoli sprouts	43 ± 9	4.525	6.67e-05 ***
10% Broccoli sprouts + 2.5% DSS	90 ± 10	9.172	7.74e-11 ***
Colon scraping			
Control + 2.5% DSS	14 ± 12	1.225	0.129
10% Broccoli sprouts	60 ± 12	5.220	1.78e-05 ***

10% Broccoli sprouts + 2.5% DSS	89 ± 12	7.749	2.81e-08 ***

252

253 **Broccoli sprouts protected against DSS-induced changes to bacterial communities**

254 Treatment was the most significant driver of bacterial community similarity in the
255 gastrointestinal tract of mice (Figure 6a,b), when considering which bacterial taxa were
256 present/absent (unweighted Jaccard Similarity, permANOVA: $F = 16.90$, $p < 0.001$) or when
257 considering presence as well as abundance (weighted Bray-Curtis Similarity, permANOVA: $F =$
258 29.97 $p < 0.001$). Mice fed a control diet clustered away from other treatments, as did mice on a
259 control diet with DSS-induced colitis, while mice on a broccoli sprout diet overlapped with mice
260 eating sprouts along with DSS-induced colitis (Figure 6a, b).

261 Using both metrics for calculating similarity, we evaluated the distance from centroids to
262 samples by treatment group (beta dispersion), as an indication of the strength of each treatment in
263 selecting bacterial communities. The Broccoli and Broccoli+DSS samples had the same amount
264 of dispersal between samples and the centroid for that treatment (beta dispersion, $p > 0.05$ for both
265 comparisons, adjusted with Tukey's Honestly Significant Difference correction for multiple
266 comparisons), while Control and Control+DSS groups had very different amounts of dispersal
267 between the samples and the centroids respective to those treatments (beta dispersion, $p < 0.05$ for
268 both comparisons, adjusted with Tukey's HSD).

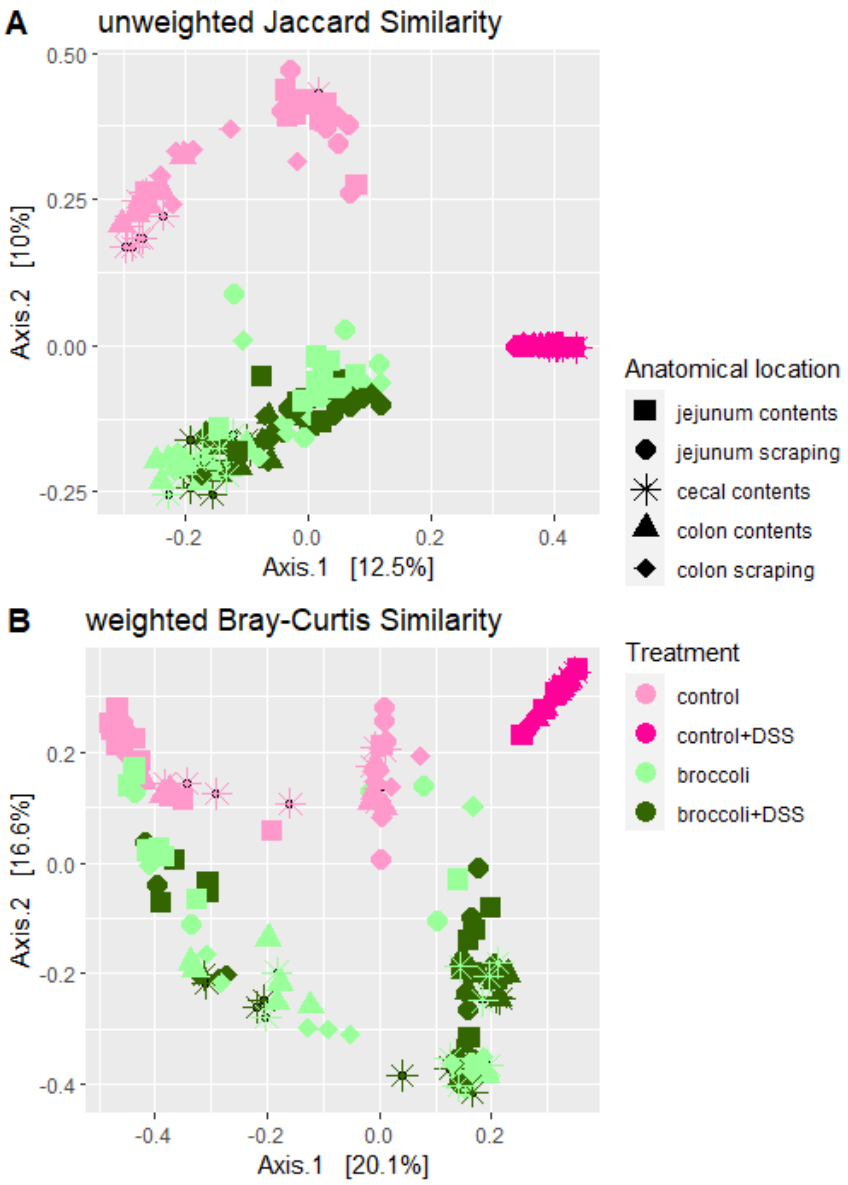

Figure 6. Principal coordinate analysis of bacterial community similarity along the intestines of mice on control diets with or without broccoli sprouts, and with or without DSS-induced chronic repeating colitis. Panel A was calculated with unweighted Jaccard Similarity to visualize differences in the taxonomic structure, and panel B with weighted Bray-Curtis to visualize structure and abundance. Four treatment groups were used in a 34-day chronic, relapsing model of colitis: control diet, control diet with DSS added to drinking water, control diet adjusted with 10% by weight steamed broccoli sprouts, and 10% broccoli sprout diet with DSS added to drinking water.

279 Within the clusters of bacterial communities for each treatment, there was a secondary
280 clustering effect of anatomical location, i.e., biogeography (Figure 7; permANOVA, uJS: $F = 3.42$,
281 $p < 0.001$; wBC: $F = 4.36$, $p < 0.001$). This is easily visualized in Control, Broccoli, and
282 Broccoli+DSS groups (Figure 6a, b), but was not observed in Control+DSS when compared with
283 the other samples. When comparing all diet treatments, the variation between the Control+DSS
284 group and the other treatments is so large that it obscures trends within the group (Figure 7a). Thus,
285 we subset the Control+DSS samples (Figure 7b), and observed that the DSS alone diminishes the
286 effect of biogeography such that there is no statistical difference (permANOVA, $p > 0.05$), except
287 marginally between jejunum scraping vs. cecum ($p = 0.04$), between anatomical locations when
288 considering the bacterial community structure (unweighted Jaccard Similarity; Figure 7b) or
289 structure and abundance (weighted Bray-Curtis, data not shown).

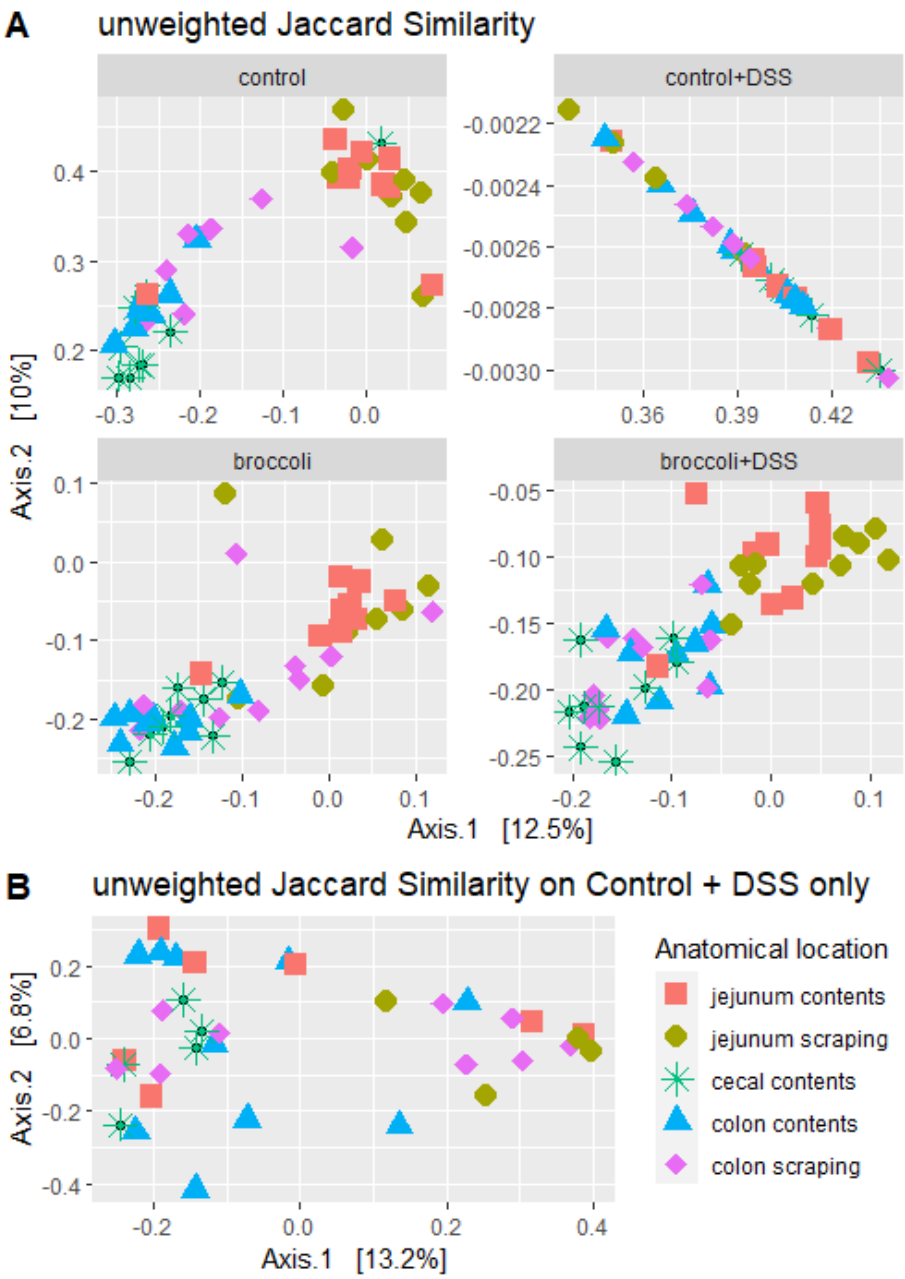

Figure 7. Principal coordinate analysis of bacterial communities from locations along the intestines of mice, across all treatments (A) and in DSS-induced colitis alone (B). Bacterial communities in the jejunum, cecum, and colon were statistically different (permANOVA, $p < 0.05$) from each other in the treatment groups (A) Control, Broccoli, and Broccoli+DSS, were not statistically different from each other after multiple bouts of colitis in the (B) Control+DSS group.

298 When identifying significant taxa which defined the samples in different treatments, there
299 were 188 significant ($p < 0.05$) features across all treatments with a permutational random forest
300 model accuracy of 98%. The Control mice contained a high abundance of mouse commensals,
301 such as *Dubosiella* spp. and strains from the Muribaculaceae and Lachnospiraceae families (Figure
302 S2). The Control+DSS mice contained much lower abundance of those known mouse commensal
303 taxa and higher abundance of the *Clostridium sensu stricto* clade (Figure S3). The Broccoli sprout
304 group was high in *Dubosiella* spp., *Parasutterella excrementihominis*, and *Bacteroides* spp.
305 (Figure S4). The Broccoli+DSS group had many of the same important taxa as the group
306 consuming Broccoli sprouts without colitis (Figure S5), implying a strong selective pressure of the
307 broccoli sprouts on the bacterial community structure such that many SVs were found in high
308 abundance across at least 70% of the samples in those mice (Figure S6). There were no bacterial
309 SVs which were shared across at least 70% of samples in the Broccoli+DSS and the Control+DSS
310 group, indicating there was not a specific community which was enriched or associated with the
311 DSS.
312

313 **Genera with putative GLR metabolism capacity present with broccoli sprout diet even**
314 **during colitis**

315 There are several bacterial taxa which are known or reputed to express myrosinase-like
316 enzymatic activity and transform glucoraphanin into sulforaphane, and we selected taxa from
317 previous literature to examine in greater detail (31, 56, 57). There were 309 bacterial SVs identified
318 to the genera *Bifidobacterium, Bacteroides, Enterococcus, Lactobacillus, Lactococcus,*
319 *Pseudomonas, Staphylococcus,* and *Streptomyces.* We found no *Faecalibacterium*, *Bacillus,*
320 *Listeria, Pediococcus, Aerobacter, Citrobacter, Enterobacter, Escherichia, Salmonella,*

321 *Paracolobactrum,* or *Proteus* in our samples (Figure 8). Only a few of these were found in Control
322 mice, with some of these genera found in the jejunum of Control+DSS mice (Figure 8), although
323 without species-level resolution it cannot be determined if these are beneficial strains.

324 Importantly, most of these reads belonged to *Bacteroides* (1,394,934 frequency across all
325 samples compared to a total frequency of 6,791 for all other sequences) and were found along the
326 gastrointestinal tract of mice consuming the broccoli sprout diet, with or without DSS (Figure 8),
327 suggesting improved GLR metabolism capacity upon the exposure to broccoli sprout diet.
328 However, for the broccoli and DSS treatment, only the cecum contents and colon scrapings
329 retained a significant proportion of *Bacteroides*. The *Bacteroides* content of the colon contents
330 appears to have been adversely affected by the addition of DSS to the broccoli diet.

331

332

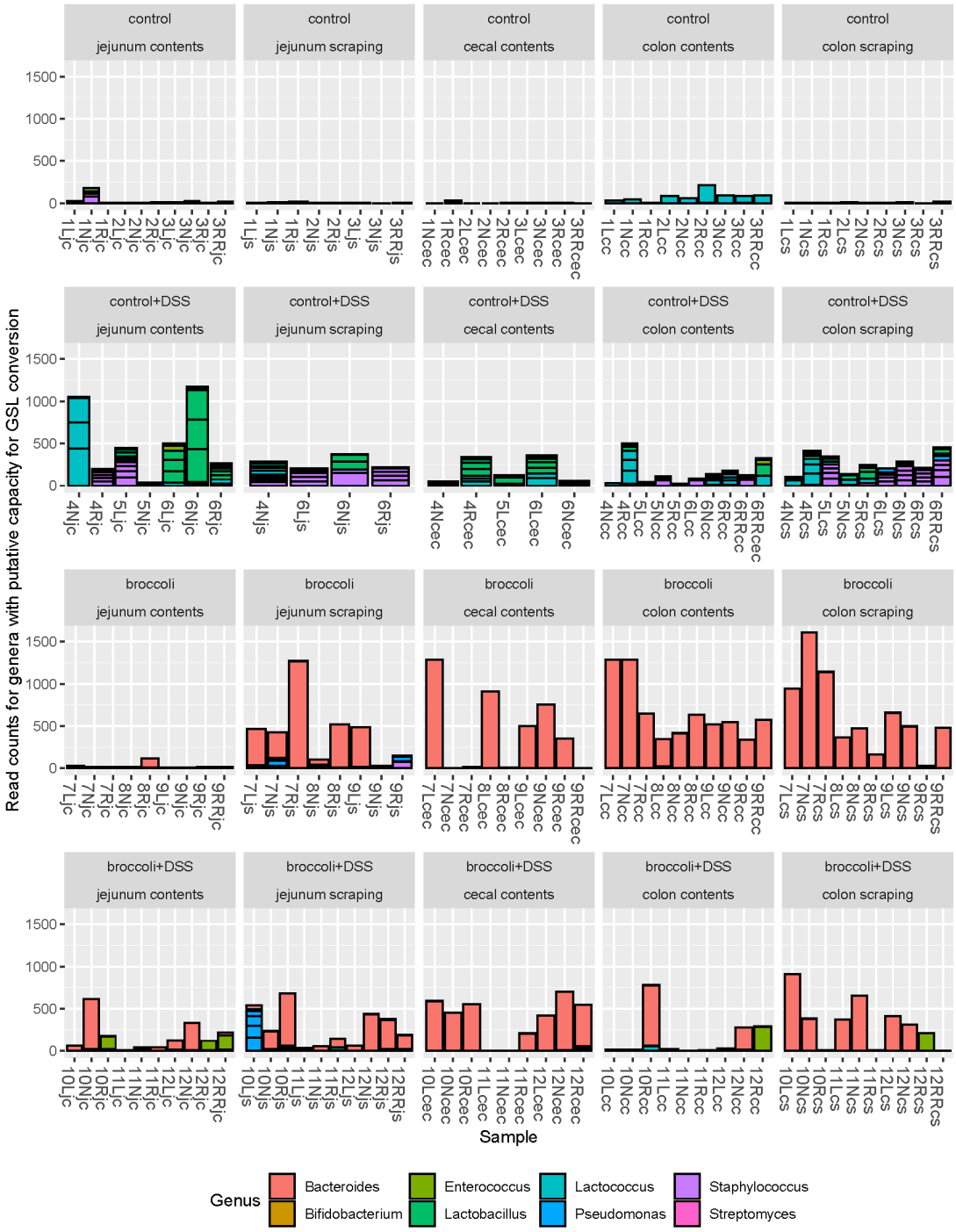

Figure 8. Bacterial sequence variants (SVs) belonging to the genera which have putative capacity to convert glucoraphanin to sulforaphane. Strains of bacteria in these genera have been demonstrated to perform myrosinase-like activity in the digestive tract, as reviewed in (56). Four treatment groups were used in a 34-day chronic, relapsing model of colitis: control diet, control diet with DSS added to drinking water, control diet adjusted with 10% by weight steamed broccoli sprouts, and 10% broccoli sprout diet with DSS added to drinking water.

342 Several *Bacteroides* species were identified (*acidifaciens*, *massiliensis*, *sartorii*), but the
343 dominant sequence variant was not identified to species-level by the Silva Database taxonomy
344 assignment (Figure 9, 10). This unidentified *Bacteroides* dominant SV (*B.*-dominant) may be
345 associated with multiple species using the NCBI Database (BLASTN): *Bacteroides*
346 *thetaiotaomicron (B. theta)*, *Bacteroides faecis* and *Bacteroides zhangwenhongiim* (all with 100%
347 Query Cover and Percent Identity). *B. theta* has been linked to myrosinase-like enzyme activity
348 and a broccoli diet, but *Bacteroides faecis* and *Bacteroides zhangwenhongii* have not.

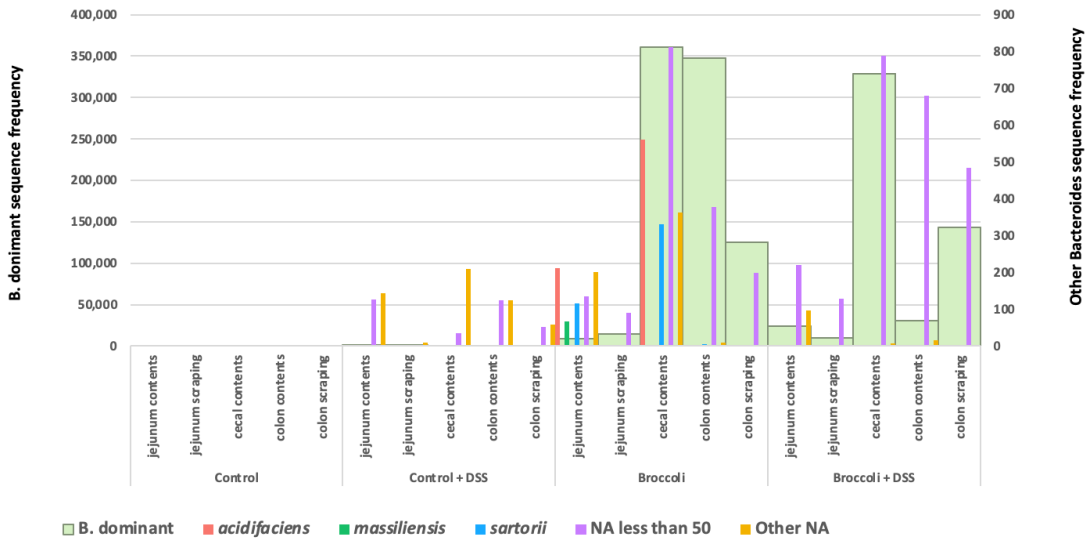

349

350 **Figure 9. Bacteroides species by diet treatment and anatomical location in the**
351 **gastrointestinal tract of mice.** The Silva Database identified *Bacteroides* species *acidifaciens*,
352 *massiliensis*, and *sartorii*. Of the BLASTN identified species for *B.*-dominant SVs, *B.*
353 *thetaiotaomicron* was the only species only found in broccoli-sprout-fed mice.

354

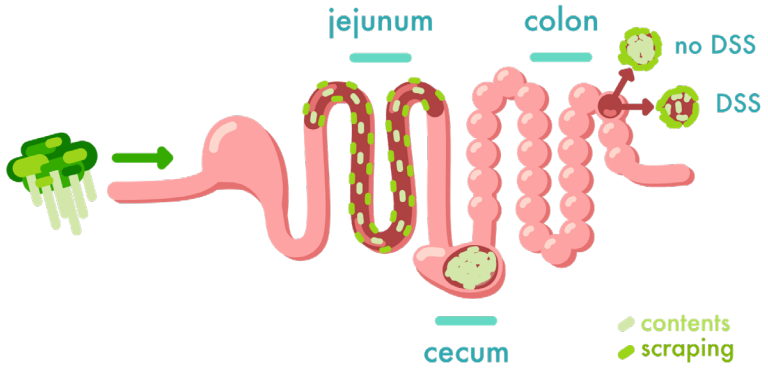

Figure 10. Biogeography of the dominant Bacillus SV, which was found exclusively in broccoli-sprout-fed mice. *B.*-dominant was present in the jejunum contents and scrapings and abundant in the cecum contents, colon contents, and colon scrapings. DSS reduced *B.*-dominant colon content density.

Discussion

Broccoli sprouts protected mice against DSS-induced colitis

The anti-inflammatory effects of broccoli and broccoli sprout bioactives, in particular sulforaphane (SFN), have been well-established in various cell, animal, and human trials of IBD (22). However, studies have not elucidated the role of the gut microbiota and the effect of biogeography in metabolizing the glucoraphanin (GLR) precursor to SFN, and the subsequent prevention and alleviation of inflammation in the gut. The present study sought to address these investigatory gaps by using a DSS-induced mouse model of chronic, relapsing colitis and comparing treatment group performance across multiple measures, including bacterial richness and abundance across treatment groups and anatomical locations, body weight, disease activity, and lipocalin analysis. We fed a 10% steamed broccoli sprout diet to SPF C57BL/6 mice beginning

374 at 6 weeks old and throughout a three-cycle regimen of DSS. Here, we showed that a diet featuring
375 10% steamed broccoli sprouts reduced the Disease Activity Index and prevented DSS-induced
376 shift in bacterial community structures along the intestines. This included preventing a shift in the
377 microbial community caused by fecal blood, which can increase the abundance of pathobionts and
378 reduce commensals (58, 59).

379 We began broccoli sprout feeding prior to introducing DSS, in part to acclimate mice to
380 the diet, but primarily to investigate the use of broccoli sprouts as a prevention strategy before the
381 initiation of colitis, as its usefulness in alleviating symptoms during active disease states has been
382 previously demonstrated (18). We chose 10% to demonstrate proof of concept and used male mice
383 as they are known to suffer more histopathological damage from DSS-induced colitis (60–62).
384 Regular access to fiber is critical to recruiting and retaining beneficial microbiota in the gut (63),
385 and regular exposure to glucosinolates is needed to stimulate gut microbial conversion (30). In
386 people sporadically consuming broccoli or broccoli sprouts, or consuming over short periods of
387 time, cooking preparation and the activity/inactivity of plant myrosinase were often the
388 determining factors in how much SFN was produced, if any, as reviewed in (30). However,
389 providing SFN directly in the diet is not feasible because it is unstable (64), and also would
390 preclude other benefits, and the enjoyability, of consuming a phenol and fiber-rich food.

391 We acknowledge that a major limitation in this study was only using male mice, as it is
392 known that hormones mediate both the gut microbiome and the type and intensity of DSS-induced
393 colitis. Thus, any future research on the application of this diet in people will require diversity in
394 the gender of participants.

395

396 **Bacterial communities are highly responsive to DSS and broccoli sprouts**

397 Mice fed broccoli sprout diets showed increased bacterial richness with and without DSS
398 compared to mice fed a control diet. We previously showed that the concentration of SFN is
399 highest in the colon after feeding C57BL/6 mice steamed broccoli sprout diets with reduced
400 myrosinase concentrations, suggesting that primary hydrolysis of SFN to GLR by microbial
401 communities occurs in the colon [32]. The current study found effects on microbial richness from
402 the broccoli sprout diet manifested most strongly in the colon, supporting our previous findings.
403 Given the location-specific dynamics of gut anatomy and physiology, digestion and the availability
404 of different nutrients, and microbial communities, a smaller change in jejunum tissues could
405 indicate that the biochemical effects of the diet are not available to the host until it reaches the
406 colon.

407 When identifying significant taxa which defined the samples in different treatments, the
408 Control mice contained a high abundance of known mouse commensal taxa, including *Dubosiella*
409 spp. and strains from the Muribaculaceae and Lachnospiraceae families. The Control+DSS mice
410 contained much lower abundance of known mouse commensal taxa and higher abundance of the
411 *Clostridium sensu stricto* clade (65), which contains known pathogens such as *Clostridium*
412 *perfringens* (66), and well-known butyrate-producing symbionts, such as *Clostridium butyricum*
413 (67).

414 The Broccoli sprout group was also high in commensal taxa such as *Dubosiella* spp., and
415 had enrichment of *Bacteroides* spp., a genus known to contain glucosinolate-metabolizing bacteria
416 and modified by cruciferous vegetable consumption (68). The broccoli sprout diet also enriched
417 for *Parasutterella excrementihominis*, which is commonly found in human murine gut
418 communities and is associated with carbohydrate intake (69). It is possible that other breakdown

419 products of glucosinolates, such as aromatic carbohydrate compounds in broccoli sprouts (70),
420 caused this enrichment. *P. excrementihominis* has also been associated with inflammation in the
421 gut in observation-based studies; however in metabolic pathway-based studies it appears to be an
422 important contributor to nitrate reduction in the gut and in reducing stress-related inflammation
423 (71). Nitrates are low in raw broccoli and other cruciferous vegetables, but this can be increased
424 by freezing (72). Thus, our diet preparation – which included freezing and freeze-drying steps –
425 may have selected for nitrate-reducers.

426 Importantly, the Broccoli+DSS group had many of the same important taxa as the group
427 consuming Broccoli sprouts without colitis, implying that the selective pressure of the broccoli
428 sprouts on the bacterial community structure may be stronger than that of the DSS. The two
429 treatments were so similar that many SVs were found in high abundance across at least 70% of the
430 samples in those mice. There were no bacterial SVs shared across at least 70% of the
431 Broccoli+DSS and the Control+DSS group, indicating there was not a specific community which
432 was enriched or associated with the DSS.

433 The inclusion of DSS in drinking water demonstrably affects mice and gut bacterial
434 communities, but it does not necessarily reduce bacterial richness. In part, this is because certain
435 bacteria, like *Proteus vulgaris,* can make use of DSS (73), while other novel commensals appear
436 to offer protective effects (74). We did not identify any bacterial SVs belonging to *Proteus*,
437 although we found significantly higher amounts of *Bacteroides* sp. in broccoli sprout-fed mice.
438 *Bacteroides thetaiotaomicron* has been demonstrated to metabolize glucoraphanin to sulforaphane
439 and offer protection against colitis in mice (31). In this experiment, for the broccoli and niche
440 microbiomes, *B.*-dominant flourished in the cecum and colon. *B.*-dominant was present under
441 broccoli treatment (no DSS) in the jejunum contents and scrapings, but was abundant in the cecum

442 contents and the colon contents and scrapings. However, for the broccoli and DSS treatment, DSS
443 presence in the colon contents did not provide as favorable an environment for *B.*-dominant.
444 Across multiple mouse lineages, individualized bacterial communities responded
445 differently to the inclusion of DSS, and the presence of *Duncaniella muricolitica* and *Alistipes*
446 *okayasuensis* were implicated in better mouse health outcomes (75). Modeling of the gut
447 microbiome indicates that certain taxa may act as keystone species – critical to building the rest of
448 the community and particularly in circumstances in which the microbial community has been
449 destabilized (76). However, no singular important bacteria has been identified in meta analyses of
450 IBD in humans (77, 78), and some studies have pointed to the switch from bacterial commensals
451 to pathobionts as important (79).
452 There is considerable evidence that microbes provide metabolism of biologically inert
453 glucosinolates to biologically active isothiocyanates, and several cultured bacterial strains from
454 fermented foods and the digestive tract have been shown to perform this conversion (31, 56, 57).
455 Additionally, a single bacterial equivalent of the plant myrosinase enzyme has not been identified,
456 and there is the possibility that several enzymes in bacteria may work in concert to achieve
457 metabolism of GSLs. Further, research is lacking to determine if the effect on the gut microbiome
458 is metabolite (isothiocyanates)-mediated or precursor (glucosinolates)-mediated. The scope of
459 research in this field should be expanded by investigating the concepts of biogeographic specificity
460 of both bioactive production and absorption and microbial community dynamics.
461

462 **Biogeography reveals location-specific trends in the bacterial community**

463 It has been well-demonstrated that distinct bacterial communities exist in different
464 locations along the gastrointestinal tract in mammals, related to the local anatomical,

465 environmental, nutritional, and host immunological conditions in different organs (36, 80, 81).
466 Further, the effect of foods on the gut microbiome can be specific to an individual's communities
467 (34). Given the complexity of microbial community function, as well as the spatially explicit
468 biochemical digestion activities of the host, it follows that the location of glucoraphanin
469 metabolism may influence how well the host can absorb SFN, whether it may be distributed
470 systematically, and where it will be effective at preventing or treating symptoms. It has previously
471 been demonstrated in mouse trials using 2,4,6 trinitrobenzene sulfonic acid to chemically induce
472 colitis that the mucosal-associated bacterial population is more affected by colitis than the lumen-
473 associated (digesta) community (43).

474 Here, we showed that DSS-induced colitis effectively erased the biogeographical
475 specificity of communities in the mouse gastrointestinal tract (Figure 4, Table 1), with the
476 exception of communities in jejunum scrapings remaining distinct from those in cecal contents.
477 Given the highly specific function of the cecum in separating fibers by size and furthering
478 microbial fermentation, it is not surprising that it would be distinct. The DSS may be a stronger
479 selective force than anatomical location in driving bacterial communities in the gut (74). For
480 example, its destruction of the epithelial cell surface may change the microarchitecture and alter
481 microbial attachment in the gut (82), and DSS increases the hydrophobicity of bile acids (83),
482 which may affect microbial survival and ability to attach to host epithelial cells, thus increasing
483 microbial washout through the gut. Any of these could possibly explain our findings that DSS
484 eliminated biogeographical specificity of communities in the mouse gastrointestinal tract.
485 However, more research would be needed to determine causation.

486 Mouse studies suggest biotransformation of glucoraphanin to SFN occurs in the colon (31,
487 44, 45), and we previously confirmed the majority of SFN accumulation takes place in the colon,

488 with greater resolution using multiple locations along the GI tract (18). Critically, the cecum had
489 low SFN, indicating that it is not responsible for hosting bacterial biotransformation of these
490 bioactives (18). Here, we also showed that only a few bacterial taxa were estimated to be sourced
491 in the cecum and creating sink populations in the colon (Figure S7), and of these, none were
492 identified to be putatively responsible for metabolism of glucoraphanin. Collectively, this confirms
493 that this is a valid model for generalization to the human gut.
494

495 **Considerations for the application of this work**

496 Access to fresh or frozen broccoli and broccoli sprouts, the cooking preparation, and the
497 ability to regularly consume these vegetables will have implications for the feasibility and success
498 of a dietary intervention for preventing or reducing inflammation in the gut. For example, sprouts
499 from various plants have been implicated in food-borne illness because of their proximity to soil,
500 and people may be wary of or discouraged from consuming raw or slightly cooked sprouts.
501 However, more recent research has shown that sprouts can be consumed safely, especially with
502 improvements in hygiene and agricultural regulations, as well as in food processing (84). Further,
503 broccoli sprouts can be grown at home in windowsill seed-bed germinators without requiring soil,
504 gardening tools, or specialized gardening knowledge, which could ease the financial burden of
505 purchasing healthy foods (85). This may prove to be particularly important in areas without access
506 to healthcare or affordable prescriptions, or in areas without close proximity to fresh, healthy fruits
507 and vegetables (7, 86, 87) as this can preclude being able to make the dietary recommendations
508 set forth by medical professionals (88). Including broccoli sprouts as 10% of the diet could be
509 potentially too high for IBD patients to comply with, and future studies on the application of this

510 diet will require a deeper understanding of the biological, microbiological, immunological, as well
511 as social and logistical factors involved in dietary interventions in people.
512
513
514 **Materials and Methods**
515 **Diet preparation**
516 Jonathan's Sprouts™ (Rochester, Massachusetts, USA) broccoli sprouts were purchased
517 from a grocery store (Bangor, Maine, USA) and steamed in a double boiler for 10 minutes and
518 immediately cooled down. They were stored in a -80°C freezer until freeze-drying (University of
519 Maine Pilot Plant, Orono, Maine, USA). The freeze-dried broccoli sprouts were ground into a fine
520 powder and mixed with purified AIN93G rodent base diet to a concentration of 10% by weight.
521 Our previous work assessed the effects of different diet preparations and the percentage of broccoli
522 sprouts, and found that 5-10% broccoli sprouts by weight reliably produces consistent anti-
523 inflammatory results in mice (18). For this study, we chose to use 10% steamed broccoli sprouts
524 both to assess the microbial conversion of GLR to SFN, and to ensure that the intervention would
525 have a strong effect. Diet pellets were formed using a silicone mold to ensure consistent sizing,
526 and allowed to dry at room temperature for up to 48 hours in a chemical safety hood to facilitate
527 moisture evaporation, and after drying were stored in sealable plastic bags in a -20°C freezer.
528
529 **DSS colitis model**
530 Forty male, 6-week-old, specific pathogen free (SPF) C57BL/6 mice (*Mus musculus*) were
531 purchased from the Jackson Laboratory (Bar Harbor, Maine, U.S.) and transferred to the animal
532 facility at the University of Maine (Orono, Maine, U.S.). The animal protocol (IACUC protocol

533 A2020-01-04) was approved by the University Committee on the Use and Care of Animals, and
534 all biosafety work was approved by the Institutional Biosafety Committee (protocol SI-092220).
535 The mice were acclimated to the facility for 7 days (day -7 to 0), during which they received *ad*
536 *libitum* autoclaved tap water and the AIN-93G purified rodent diet (control diet). After initial
537 acclimation, the mice were randomly assigned to one of 4 experimental groups beginning on
538 experimental day 0: control diet without DSS treatment (Control), 10% steamed broccoli sprout
539 diet without DSS treatment (Broccoli), control diet with DSS treatment (Control+DSS), and 10%
540 steamed broccoli sprout diet with DSS treatment (Broccoli+DSS). All experimental groups were
541 on 7 days of their respective diets (control or 10% steamed broccoli sprout), after which DSS (Alfa
542 Aesar, molecular weight ~40 kD (53)) was added to the drinking water of the DSS treatment
543 groups to a final concentration of 2.5%. Mice were given DSS for 5 days, followed by a recovery
544 period for 5 - 7 days. This was repeated for a total of 3 cycles to induce chronic colitis (48, 89).
545 Mice were sacrificed and tissue collected after the third round of DSS, on day 35 of the experiment.
546 Bodyweight, fecal blood, and fecal consistency were used to calculate Disease Activity
547 Index (DAI) scores (52). Samples were taken every 2 - 3 days throughout the trial, and daily during
548 the DSS cycles. Body weights and DAI were analyzed using 2-way ANOVA generated with R to
549 compare differences between treatments for each day. A generalized additive model (GAM) was
550 used in R to compare DAI differences (R-sq.(adj) = 0.861, Deviance explained = 86.4%, GCV =
551 0.036031) by treatment across the entire study, using Mouse ID to account for repeated measures.
552 Lipocalin-2 concentration in the plasma and fecal samples were determined by a mouse Lipocalin-
553 2/NGAL DuoSet ELISA kit (R & D Biosystems, USA) following the manufacturer's instructions.
554 Lipocalin is a neutrophil protein that binds bacterial siderophores and serves as a surrogate marker
555 for intestinal inflammation in IBD (90). The readings at wavelengths of 540 nm and 450 nm were

556 measured by a Thermo Scientific Varioskan LUX Multimode Microplate Reader. The readings at
557 540 nm were subtracted from the readings at 450 nm to correct for the discoloration of the solution.
558 After euthanasia, lumen-associated (digesta contents) and mucosal-associated (epithelial
559 scrapings) microbial community samples were collected from the jejunum, cecum (contents only),
560 and colon for DNA extraction and community sequencing as described below.
561
562 **Bacterial community sequencing and analysis**
563 From the DSS mice, digesta (lumen contents) and epithelial associated (tissue scrapings)
564 microbial community samples were collected from the jejunum, cecum (contents only), and colon.
565 All tissues containing their resident gut microbiota were gently homogenized with vortexing, then
566 treated with propidium monoazide (PMA; BioTium) following kit protocols at a final
567 concentration of 25 µm. PMA covalently binds to relic/free DNA and DNA inside
568 compromised/dead cell membranes, and prevents amplification in downstream protocols to
569 preclude dead DNA from the sequence data (91).
570 Following PMA treatment, bulk DNA was extracted from tissue-associated bacterial
571 communities (n = 200 samples), or no-template (water) control samples (n = 10, one for each
572 extraction batch) using commercially available kits optimized for water and tissue-based microbial
573 communities (Quick-DNA Fecal/Soil Kit, Zymo Research). DNA extract was roughly quantified
574 and purity-checked with a Thermo Scientific™ NanoDrop™ OneC Microvolume UV-Vis
575 Spectrophotometer (Thermo Scientific, Waltham, MA, U.S.). Samples underwent DNA amplicon
576 sequencing of the 16S rRNA gene V3-V4 region, using primers 341F [174] and 806R [175] and
577 protocols consistent with The Earth Microbiome Project [176], and sequenced on an Illumina
578 MiSeq platform using the 2 x 300-nt V3 kit (Molecular Research Labs, Clearwater, TX, U.S.).

579 Raw sequence data (fastq files and metadata) is available from NCBI through BioProject
580 Accession number PRJNA911821.

581 Amplicon sequence data was processed using previously curated workflows in the Ishaq
582 Lab (R code supplied as Supplemental Material), which used the DADA2 pipeline ver. 1.26
583 (DADA2 Pipeline Tutorial (1.4), 2016.) in the R software environment ver. 4.1.1 [177]. The
584 dataset started with 46,581,832 paired raw reads, and based on initial quality assessment only the
585 forward reads were processed. Trimming parameters were designated based on visual assessment
586 of the aggregated quality scores at each base from all samples (plotQualityProfile in DADA2): the
587 first 10 bases were trimmed, sequences were trimmed to 225 bases in length, and were discarded
588 if they had ambiguous bases, more than two errors, or matched the PhiX version 3 positive control
589 (Illumina; FC-110-3001). After filtering, 34,009,802 non-unique forward/read 1 sequences
590 remained.

591 The DADA algorithm was used to estimate the error rates for the sequencing run,
592 dereplicate the reads, pick sequence variants (SVs) which represent 'microbial individuals', and
593 remove chimeric artifacts from the sequence table. Taxonomy was assigned using the Silva
594 taxonomic training data version 138.1 [178] down to species where possible, and reads matching
595 chloroplasts and mitochondria taxa were removed using the dplyr package [179]. No-template
596 control samples were used to remove contaminating sequences from the samples by extraction
597 batch [180]. The sequence table, taxonomy, and metadata were combined for each experiment
598 using the phyloseq package [181], which was also used for basic visualization and statistical
599 analysis in combination with other packages. Samples from one mouse (4L, in the Control+DSS
600 group) were dropped from further analysis as they were outliers on all visualizations and may have
601 been contaminated during DNA extraction.

602 Normality was checked using a Shapiro-Wilkes test on alpha diversity metrics generated
603 from rarefied data, including observed richness, evenness, and Shannon diversity. Linear models
604 were run for comparisons of alpha diversity metrics to compare by sample type, (lme4 package
605 [182]), in which anatomical location and diet treatment were used as fixed effects, and mouse ID
606 used to control for repeated sampling as needed. Generalized additive models were used to assess
607 trends in alpha diversity using time as a smoother (92). Jaccard unweighted similarity was used to
608 calculate sample similarity based on community membership (species presence/absence),
609 visualized with non-parametric multidimensional scaling, and tested with permutational analysis
610 of variance (permANOVA) by using the vegan package (93). Random forest feature prediction
611 with permutation was used to identify differentially abundant SVs based on factorial conditions
612 (94). Plots were made using the ggplot2 (95), ggpubr (96), and phyloseq packages.
613 Source Tracker algorithms which had been modified for the R platform (97, 98) were used
614 to identify source:sink effects based on anatomical location. This was used to determine if the
615 cecum could be the source for population sinks in the colon, as a proxy for the model's applicability
616 to the human gut anatomical features and microbial communities. A total of 142 SVs were
617 identified as possibly sourced from the cecum, and 95 SVs were estimated to make up >1% of the
618 proportion of sources (Figure S7). The putative GLR converting bacteria in the Broccoli and
619 Broccoli+DSS mouse gut samples were not among those taxa identified as sourced in the cecum.
620
621
622 **Acknowledgements**
623
624 All authors have read and approved the final manuscript. The authors thank Jess Majors,
625 University of Maine, for her kind and detailed care of the mice during the trial, and for Ellie
626 Pelletier for her informal review of the manuscript. This project was supported by the USDA

National Institute of Food and Agriculture through the Maine Agricultural & Forest Experiment Station: Hatch Project Numbers ME022102 and ME022329 (Ishaq) and ME022303 (Li); the USDA-NIFA-AFRI Foundational Program [Li and Chen; USDA/NIFA 2018-67017-27520/2018-67017-36797]; and the National Institute of Health [Li and Ishaq; NIH/NIDDK 1R15DK133826-01]. Johanna Holman was supported by ME0-22303 (Li), and Lola Holcomb was supported by US National Science Foundation One Health and the Environment (OG&E): Convergence of Social and Biological Sciences NRT program grant DGE-1922560, and through the UMaine Graduate School of Biomedical Sciences and Engineering.

Author Contributions

Conceptualization, S.L.I., Y.L., T.Z., G.C., G.M; Methodology, S.L.I., Y.L., T.Z., G.M., P.M., J.H.; Software, S.L.I.; Formal Analysis, J.H., S.L.I., T.H., B.H.; Investigation, J.H., L.C., J.B.; G.C., D.B.; Resources, S.L.I., Y.L., T.Z.; Data Curation, S.L.I., J.H.; Writing - Original Draft, J.H., L.C., S.L.I., Y.L.; Writing - Review and Editing; S.L.I., Y.L., T.Z., G.M., P.M., J.H., L.C., J.B., G.C., D.B., T.H., B.H., L.H.; Visualization, J.H., S.L.I., T.H., B.H.; Supervision, J.H., S.L.I., Y.L., T.Z.; Project Administration, S.L.I., Y.L., T.Z; Funding Acquisition, S.L.I., Y.L., T.Z., G.C.

Figure Legends

Figure 1. Experimental design schematic for a chronic model of colitis induced by dextran sodium sulfate (DSS) in 40 male mice (C57BL/6) beginning at 6-weeks of age.

Figure 2. Metrics of disease status in a DSS-Induced model of chronic colitis, including (A) mouse body weights and (B) Disease Activity Index, by day of experiment. Body weights and time scale were normalized to the day mice began the broccoli sprout diet. DAI scores are calculated by weight loss intensity score, fecal blood, and fecal consistency. Treatment comparisons at each day compared by ANOVA, and significance is designated as 0 - 0.001 '***'. Four treatment groups were used in a 34-day chronic, relapsing model of colitis: control diet, control diet with DSS added to drinking water, control diet adjusted with 10% by weight steamed broccoli sprouts, and 10% broccoli sprout diet with DSS added to drinking water.

659 **Figure 3 Lipocalin in (A) feces at multiple timepoints and (B) serum on the last day of the**
660 **trial from mice in a DSS-Induced model of chronic colitis.** Significance was determined as p
661 < 0.05, ANOVA.

662 **Figure 4. Gut bacterial taxa identified from mice receiving DSS which were associated with**
663 **having a positive fecal occult blood score on the last day of the experiment, by treatment.**
664 Data were subset to mice with a positive score on the last day of the experiment, when the gut
665 samples were collected. Important features (SVs) were identified through permutational random
666 forest analysis, and only the features important to this group (>50 reads) are listed out of 143
667 significant ($p < 0.05$) features across all treatments. Model accuracy was 89.7%. Bacterial
668 sequence variants (SV) are identified as the lowest level of taxonomic identity possible, with "NA"
669 indicating which could not be identified to species, and the number indicating which specific SV
670 it was. Four treatment groups were used in a 34-day chronic, relapsing model of colitis, those
671 included here are a control diet with DSS added to drinking water, and 10% broccoli sprout diet
672 with DSS added to drinking water.

673 **Figure 5. Observed bacterial richness along the intestinal of mice on control diets with or**
674 **without broccoli sprouts, and with or without DSS-induced chronic repeating colitis.**
675 Richness is calculated as the number of different bacterial sequence variants (SVs). Statistically
676 significant comparisons are provided in Table 1. Four treatment groups were used in a 34-day
677 chronic, relapsing model of colitis: control diet, control diet with DSS added to drinking water,
678 control diet adjusted with 10% by weight steamed broccoli sprouts, and 10% broccoli sprout diet
679 with DSS added to drinking water.
680 **Figure 6. Principal coordinate analysis of bacterial community similarity along the**
681 **intestines of mice on control diets with or without broccoli sprouts, and with or without**
682 **DSS-induced chronic repeating colitis.** Panel A was calculated with unweighted Jaccard
683 Similarity to visualize differences in the taxonomic structure, and panel B with weighted Bray-
684 Curtis to visualize structure and abundance. Four treatment groups were used in a 34-day
685 chronic, relapsing model of colitis: control diet, control diet with DSS added to drinking water,
686 control diet adjusted with 10% by weight steamed broccoli sprouts, and 10% broccoli sprout diet
687 with DSS added to drinking water.
688
689 **Figure 7. Principal coordinate analysis of bacterial communities from locations along the**
690 **intestines of mice, across all treatments (A) and in DSS-induced colitis alone (B).** Bacterial
691 communities in the jejunum, cecum, and colon were statistically different (permANOVA, p <
692 0.05) from each other in the treatment groups (A) Control, Broccoli, and Broccoli+DSS, were
693 not statistically different from each other after multiple bouts of colitis in the (B) Control+DSS
694 group.
695
696 **Figure 8. Bacterial sequence variants (SVs) belonging to the genera which have putative**
697 **capacity to convert glucoraphanin to sulforaphane.** Strains of bacteria in these genera have
698 been demonstrated to perform myrosinase-like activity in the digestive tract, as reviewed in (56).

699 Four treatment groups were used in a 34-day chronic, relapsing model of colitis: control diet,
700 control diet with DSS added to drinking water, control diet adjusted with 10% by weight steamed
701 broccoli sprouts, and 10% broccoli sprout diet with DSS added to drinking water.
702
703 **Figure 9. Bacteroides species by diet treatment and anatomical location in the**
704 **gastrointestinal tract of mice.** The Silva Database identified *Bacteroides* species *acidifaciens*,
705 *massiliensis*, and *sartorii*. Of the BLASTN identified species for *B.*-dominant SVs*, B.*
706 *thetaiotaomicron* was the only species only found in broccoli-sprout-fed mice.
707
708
709 **Figure 10. Biogeography of the dominant Bacillus SV, which was found exclusively in**
710 **broccoli-sprout-fed mice.** *B.*-dominant was present in the jejunum contents and scrapings and
711 abundant in the cecum contents, colon contents, and colon scrapings. DSS reduced *B.*-dominant
712 colon content density.
713

714 **References**

715 1. Peery AF, Crockett SD, Murphy CC, Lund JL, Dellon ES, Williams JL, Jensen ET,
716 Shaheen NJ, Barritt AS, Lieber SR, Kochar B, Barnes EL, Fan YC, Pate V, Galanko J,
717 Baron TH, Sandler RS. 2019. Burden and Cost of Gastrointestinal, Liver, and Pancreatic
718 Diseases in the United States: Update 2018. Gastroenterology 156:254–272.e11.

719 2. Singh S, Qian AS, Nguyen NH, Ho SKM, Luo J, Jairath V, Sandborn WJ, Ma C. 2022.
720 Trends in U.S. Health Care Spending on Inflammatory Bowel Diseases, 1996-2016.
721 Inflamm Bowel Dis 28:364–372.

722 3. Klampfer L. 2013. Cytokines, inflammation and colon cancer. Current Cancer Drug Targets
723 11:451–464.

724 4. Zhang Y-Z. 2014. Inflammatory bowel disease: Pathogenesis. World J Gastroenterol 20:91.

725 5. Matricon J, Barnich N, Ardid D. 2010. Immunopathogenesis of inflammatory bowel
726 disease. Self Nonself 1:299–309.

727 6. Rubin DC, Shaker A, Levin MS. 2012. Chronic intestinal inflammation: Inflammatory
728 bowel disease and colitis-associated colon cancer. Frontiers in Immunology 3:00107.

729 7. Walker RE, Keane CR, Burke JG. 2010. Disparities and access to healthy food in the
730 United States: A review of food deserts literature. Health Place 16:876–884.

731 8. Banerjee S, Ghosh S, Sinha K, Chowdhury S, Sil PC. 2019. Sulphur dioxide ameliorates
732 colitis related pathophysiology and inflammation. Toxicology 412:63–78.

733 9. Lewis JD, Abreu MT. 2017. Diet as a Trigger or Therapy for Inflammatory Bowel Diseases.

734 Gastroenterology 152:398–414.e6.

735 10. Armstrong HK, Bording-Jorgensen M, Santer DM, Zhang Z, Valcheva R, Rieger AM,
736 Sung-Ho Kim J, Dijk SI, Mahmood R, Ogungbola O, Jovel J, Moreau F, Gorman H,
737 Dickner R, Jerasi J, Mander IK, Lafleur D, Cheng C, Petrova A, Jeanson T-L, Mason A,
738 Sergi CM, Levine A, Chadee K, Armstrong D, Rauscher S, Bernstein CN, Carroll MW,
739 Huynh HQ, Walter J, Madsen KL, Dieleman LA, Wine E. 2022. Unfermented β-fructan
740 Fibers Fuel Inflammation in Select Inflammatory Bowel Disease Patients. Gastroenterology
741 https://doi.org/10.1053/j.gastro.2022.09.034.

742 11. Tse G, Eslick GD. 2014. Cruciferous vegetables and risk of colorectal neoplasms: a
743 systematic review and meta-analysis. Nutr Cancer 66:128–139.

744 12. Huang L, Li B-L, He C-X, Zhao Y-J, Yang X-L, Pang B, Zhang X-H, Shan Y-J. 2018.
745 Sulforaphane inhibits human bladder cancer cell invasion by reversing epithelial-to-
746 mesenchymal transition via directly targeting microRNA-200c/ZEB1 axis. J Funct Foods
747 41:118–126.

748 13. Li Y, Wicha MS, Schwartz SJ, Sun D. 2011. Implications of cancer stem cell theory for
749 cancer chemoprevention by natural dietary compounds. J Nutr Biochem 22:799–806.

750 14. Li Y, Zhang T, Schwartz SJ, Sun D. 2011. Sulforaphane Potentiates the Efficacy of 17-
751 Allylamino 17-Demethoxygeldanamycin Against Pancreatic Cancer Through Enhanced
752 Abrogation of Hsp90 Chaperone Function. Nutrition and Cancer
753 https://doi.org/10.1080/01635581.2011.596645.

754 15. Li Y, Zhang T, Korkaya H, Liu S, Lee H-F, Newman B, Yu Y, Clouthier SG, Schwartz SJ,

755 Wicha MS, Sun D. 2010. Sulforaphane, a dietary component of broccoli/broccoli sprouts,
756 inhibits breast cancer stem cells. Clin Cancer Res 16:2580–2590.

757 16. Angelino D, Jeffery E. 2014. Glucosinolate hydrolysis and bioavailability of resulting
758 isothiocyanates: Focus on glucoraphanin. J Funct Foods 7:67–76.

759 17. Shapiro TA, Fahey JW, Wade KL, Stephenson KK, Talalay P. 1998. Human metabolism
760 and excretion of cancer chemoprotective glucosinolates and isothiocyanates of cruciferous
761 vegetables. Cancer Epidemiol Biomarkers Prev 7:1091–1100.

762 18. Zhang T, Holman J, McKinstry D, Trindade BC, Eaton KA, Mendoza-Castrejon J, Ho S,
763 Wells E, Yuan H, Wen B, Sun D, Chen GY, Li Y. 2022. A steamed broccoli sprout diet
764 preparation that reduces colitis via the gut microbiota. J Nutr Biochem 112:109215.

765 19. Fahey JW, Stephenson KK, Wade KL, Talalay P. 2013. Urease from *Helicobacter pylori* is
766 inactivated by sulforaphane and other isothiocyanates. Biochem Biophys Res Commun
767 435:1–7.

768 20. Fahey JW, Wehage SL, Holtzclaw WD, Kensler TW, Egner PA, Shapiro TA, Talalay P.
769 2012. Protection of humans by plant glucosinolates: efficiency of conversion of
770 glucosinolates to isothiocyanates by the gastrointestinal microflora. Cancer Prev Res (Phila)
771 5:603–611.

772 21. Wei L-Y, Zhang J-K, Zheng L, Chen Y. 2022. The functional role of sulforaphane in
773 intestinal inflammation: a review. Food Funct 13:514–529.

774 22. Holman J, Hurd M, Moses P, Mawe G, Zhang T, Ishaq SL, Li Y. 2023. Interplay of

775 Broccoli/Broccoli Sprout Bioactives with Gut Microbiota in Reducing Inflammation in
776 Inflammatory Bowel Diseases. J Nutr Biochem 113:109238.

777 23. Sun C-C, Li S-J, Yang C-L, Xue R-L, Xi Y-Y, Wang L, Zhao Q-L, Li D-J. 2015.
778 Sulforaphane attenuates muscle inflammation in dystrophin-deficient mdx mice via NF-E2-
779 related factor 2 (Nrf2)-mediated inhibition of NF-κB signaling pathway. J Biol Chem
780 290:17784–17795.

781 24. Petkovic M, Leal EC, Alves I, Bose C, Palade PT, Singh P, Awasthi S, Børsheim E,
782 Dalgaard LT, Singh SP, Carvalho E. 2021. Dietary supplementation with sulforaphane
783 ameliorates skin aging through activation of the Keap1-Nrf2 pathway. J Nutr Biochem
784 98:108817.

785 25. Mazarakis N, Snibson K, Licciardi PV, Karagiannis TC. 2020. The potential use of l-
786 sulforaphane for the treatment of chronic inflammatory diseases: A review of the clinical
787 evidence. Clin Nutr 39:664–675.

788 26. Zhang Y, Tan L, Li C, Wu H, Ran D, Zhang Z. 2020. Sulforaphane alter the microbiota and
789 mitigate colitis severity on mice ulcerative colitis induced by DSS. AMB Express 10:119.

790 27. Liu X, Wang Y, Hoeflinger JL, Neme BP, Jeffery EH, Miller MJ. 2017. Dietary Broccoli
791 Alters Rat Cecal Microbiota to Improve Glucoraphanin Hydrolysis to Bioactive
792 Isothiocyanates. Nutrients 9.

793 28. Manichanh C, Rigottier-Gois L, Bonnaud E, Gloux K, Pelletier E, Frangeul L, Nalin R,
794 Jarrin C, Chardon P, Marteau P, Roca J, Dore J. 2006. Reduced diversity of faecal
795 microbiota in Crohn's disease revealed by a metagenomic approach. Gut 55:205–211.

796 29. Palop ML, LLanos Palop M, Smiths JP, ten Brink B. 1995. Degradation of sinigrin by
797 *Lactobacillus agilis* strain R16. International Journal of Food Microbiology
798 https://doi.org/10.1016/0168-1605(95)00123-2.

799 30. Angelino D, Dosz EB, Sun J, Hoeflinger JL, Van Tassell ML, Chen P, Harnly JM, Miller
800 MJ, Jeffery EH. 2015. Myrosinase-dependent and -independent formation and control of
801 isothiocyanate products of glucosinolate hydrolysis. Front Plant Sci 6:831.

802 31. Liou CS, Sirk SJ, Diaz CAC, Klein AP, Fischer CR, Higginbottom SK, Erez A, Donia MS,
803 Sonnenburg JL, Sattely ES. 2020. A Metabolic Pathway for Activation of Dietary
804 Glucosinolates by a Human Gut Symbiont. Cell 180:717–728.e19.

805 32. Elfoul L, Rabot S, Khelifa N, Quinsac A, Duguay A, Rimbault A. 2001. Formation of allyl
806 isothiocyanate from sinigrin in the digestive tract of rats monoassociated with a human
807 colonic strain of *Bacteroides thetaiotaomicron*. FEMS Microbiol Lett 197:99–103.

808 33. Singh RK, Chang H-W, Yan D, Lee KM, Ucmak D, Wong K, Abrouk M, Farahnik B,
809 Nakamura M, Zhu TH, Bhutani T, Liao W. 2017. Influence of diet on the gut microbiome
810 and implications for human health. J Transl Med 15:73.

811 34. Johnson AJ, Vangay P, Al-Ghalith GA, Hillmann BM, Ward TL, Shields-Cutler RR, Kim
812 AD, Shmagel AK, Syed AN, Personalized Microbiome Class Students, Walter J, Menon R,
813 Koecher K, Knights D. 2019. Daily Sampling Reveals Personalized Diet-Microbiome
814 Associations in Humans. Cell Host Microbe 25:789–802.e5.

815 35. Amato KR, Arrieta M-C, Azad MB, Bailey MT, Broussard JL, Bruggeling CE, Claud EC,
816 Costello EK, Davenport ER, Dutilh BE, Swain Ewald HA, Ewald P, Hanlon EC, Julion W,

817 Keshavarzian A, Maurice CF, Miller GE, Preidis GA, Segurel L, Singer B, Subramanian S,
818 Zhao L, Kuzawa CW. 2021. The human gut microbiome and health inequities. Proc Natl
819 Acad Sci U S A 118:e2017947118.

820 36. Tropini C, Earle KA, Huang KC, Sonnenburg JL. 2017. The Gut Microbiome: Connecting
821 Spatial Organization to Function. Cell Host Microbe 21:433–442.

822 37. Hillman ET, Lu H, Yao T, Nakatsu CH. 2017. Microbial Ecology along the Gastrointestinal
823 Tract. Microbes Environ 32:300–313.

824 38. Lynch SV, Pedersen O. 2016. The Human Intestinal Microbiome in Health and Disease. N
825 Engl J Med 375:2369–2379.

826 39. Press AG, Hauptmann IA, Hauptmann L, Fuchs B, Fuchs M, Ewe K, Ramadori G. 1998.
827 Gastrointestinal pH profiles in patients with inflammatory bowel disease. Aliment
828 Pharmacol Ther 12:673–678.

829 40. Compare D, Pica L, Rocco A, De Giorgi F, Cuomo R, Sarnelli G, Romano M, Nardone G.
830 2011. Effects of long-term PPI treatment on producing bowel symptoms and SIBO.
831 European Journal of Clinical Investigation https://doi.org/10.1111/j.1365-
832 2362.2010.02419.x.

833 41. Swidsinski A, Ladhoff A, Pernthaler A, Swidsinski S, Loening-Baucke V, Ortner M, Weber
834 J, Hoffmann U, Schreiber S, Dietel M, Lochs H. 2002. Mucosal flora in inflammatory
835 bowel disease. Gastroenterology 122:44–54.

836 42. Gevers D, Kugathasan S, Denson LA, Vázquez-Baeza Y, Van Treuren W, Ren B, Schwager

837 E, Knights D, Song SJ, Yassour M, Morgan XC, Kostic AD, Luo C, González A,
838 McDonald D, Haberman Y, Walters T, Baker S, Rosh J, Stephens M, Heyman M,
839 Markowitz J, Baldassano R, Griffiths A, Sylvester F, Mack D, Kim S, Crandall W, Hyams
840 J, Huttenhower C, Knight R, Xavier RJ. 2014. The treatment-naive microbiome in new-
841 onset Crohn's disease. Cell Host Microbe 15:382–392.

842 43. Kozik AJ, Nakatsu CH, Chun H, Jones-Hall YL. 2019. Comparison of the fecal, cecal, and
843 mucus microbiome in male and female mice after TNBS-induced colitis. PLoS One
844 14:e0225079.

845 44. Lai R-H, Miller MJ, Jeffery E. 2010. Glucoraphanin hydrolysis by microbiota in the rat
846 cecum results in sulforaphane absorption. Food Funct 1:161–166.

847 45. Li F, Hullar MAJ, Beresford SAA, Lampe JW. 2011. Variation of glucoraphanin
848 metabolism in vivo and ex vivo by human gut bacteria. Br J Nutr 106:408–416.

849 46. Eichele DD, Kharbanda KK. 2017. Dextran sodium sulfate colitis murine model: An
850 indispensable tool for advancing our understanding of inflammatory bowel diseases
851 pathogenesis. World J Gastroenterol 23:6016–6029.

852 47. Okayasu I, Hatakeyama S, Yamada M, Ohkusa T, Inagaki Y, Nakaya R. 1990. A novel
853 method in the induction of reliable experimental acute and chronic ulcerative colitis in mice.
854 Gastroenterology 98:694–702.

855 48. Wirtz S, Popp V, Kindermann M, Gerlach K, Weigmann B, Fichtner-Feigl S, Neurath MF.
856 2017. Chemically induced mouse models of acute and chronic intestinal inflammation. Nat
857 Protoc 12:1295–1309.

858 49. Poritz LS, Garver KI, Green C, Fitzpatrick L, Ruggiero F, Koltun WA. 2007. Loss of the
859 tight junction protein ZO-1 in dextran sulfate sodium induced colitis. J Surg Res 140:12–19.

860 50. Chassaing B, Aitken JD, Malleshappa M, Vijay-Kumar M. 2014. Dextran sulfate sodium
861 (DSS)-induced colitis in mice. Curr Protoc Immunol 104:15.25.1–15.25.14.

862 51. Araki A, Kanai T, Ishikura T, Makita S, Uraushihara K, Iiyama R, Totsuka T, Takeda K,
863 Akira S, Watanabe M. 2005. MyD88-deficient mice develop severe intestinal inflammation
864 in dextran sodium sulfate colitis. J Gastroenterol 40:16–23.

865 52. Dieleman LA, Ridwan BU, Tennyson GS, Beagley KW, Bucy RP, Elson CO. 1994.
866 Dextran sulfate sodium-induced colitis occurs in severe combined immunodeficient mice.
867 Gastroenterology 107:1643–1652.

868 53. da Costa Goncalves F, Schneider N, Mello HF, Passos EP, da Rosa Paz AH. 2013.
869 Characterization of Acute Murine Dextran Sodium Sulfate (DSS) Colitis: Severity of
870 Inflammation is Dependent on the DSS Molecular Weight and Concentration. Acta
871 Scientiae Veterinari 41:1–9.

872 54. Breynaert C, Dresselaers T, Cremer J, Van Steen K, Perrier C, Vermeire S, Rutgeerts P,
873 Ceuppens J, Himmelreich U, Van Assche G. 2012. P024 Repeated cycles of DSS inducing a
874 chronically relapsing inflammation: A novel model to study fibrosis using in vivo MRI T2
875 relaxometry. J Crohns Colitis 6:S20.

876 55. Delage C, Taib T, Mamma C, Lerouet D, Besson VC. 2021. Traumatic Brain Injury: An
877 Age-Dependent View of Post-Traumatic Neuroinflammation and Its Treatment.
878 Pharmaceutics 13:1624.

879 56. Sikorska-Zimny K, Beneduce L. 2021. The Metabolism of Glucosinolates by Gut
880 Microbiota. Nutrients 13:2750.

881 57. Luang-In V, Narbad A, Cebeci F, Bennett M, Rossiter JT. 2015. Identification of Proteins
882 Possibly Involved in Glucosinolate Metabolism in *L. agilis* R16 and *E. coli* VL8. Protein J
883 34:135–146.

884 58. Chénard T, Malick M, Dubé J, Massé E. 2020. The influence of blood on the human gut
885 microbiome. BMC Microbiol 20:44.

886 59. Cafiero C, Re A, Pisconti S, Trombetti M, Perri M, Colosimo M, D'Amato G, Gallelli L,
887 Cannataro R, Molinario C, Fazio A, Caroleo MC, Cione E. 2020. Dysbiosis in intestinal
888 microbiome linked to fecal blood determined by direct hybridization. 3 Biotech 10:358.

889 60. Mähler M, Bristol IJ, Leiter EH, Workman AE, Birkenmeier EH, Elson CO, Sundberg JP.
890 1998. Differential susceptibility of inbred mouse strains to dextran sulfate sodium-induced
891 colitis. Am J Physiol 274:G544–51.

892 61. Bábíčková J, Tóthová Ľ, Lengyelová E, Bartoňová A, Hodosy J, Gardlík R, Celec P. 2015.
893 Sex Differences in Experimentally Induced Colitis in Mice: a Role for Estrogens.
894 Inflammation 38:1996–2006.

895 62. Goodman WA, Havran HL, Quereshy HA, Kuang S, De Salvo C, Pizarro TT. 2018.
896 Estrogen Receptor α Loss-of-Function Protects Female Mice From DSS-Induced
897 Experimental Colitis. Cell Mol Gastroenterol Hepatol 5:630–633.e1.

898 63. Letourneau J, Holmes ZC, Dallow EP, Durand HK, Jiang S, Carrion VM, Gupta SK,

899 Mincey AC, Muehlbauer MJ, Bain JR, David LA. 2022. Ecological memory of prior
900 nutrient exposure in the human gut microbiome. ISME J 16:2479–2490.

901 64. Yagishita Y, Fahey JW, Dinkova-Kostova AT, Kensler TW. 2019. Broccoli or
902 Sulforaphane: Is It the Source or Dose That Matters? Molecules 24:3593.

903 65. Stackebrandt E, Kramer I, Swiderski J, Hippe H. 1999. Phylogenetic basis for a taxonomic
904 dissection of the genus *Clostridium*. FEMS Immunol Med Microbiol 24:253–258.

905 66. Uzal FA, McClane BA, Cheung JK, Theoret J, Garcia JP, Moore RJ, Rood JI. 2015. Animal
906 models to study the pathogenesis of human and animal *Clostridium perfringens* infections.
907 Vet Microbiol 179:23–33.

908 67. Chen H, Ma X, Liu Y, Ma L, Chen Z, Lin X, Si L, Ma X, Chen X. 2019. Gut Microbiota
909 Interventions With *Clostridium butyricum* and Norfloxacin Modulate Immune Response in
910 Experimental Autoimmune Encephalomyelitis Mice. Front Immunol 10:1662.

911 68. Shahinozzaman M, Raychaudhuri S, Fan S, Obanda DN. 2021. Kale Attenuates
912 Inflammation and Modulates Gut Microbial Composition and Function in C57BL/6J Mice
913 with Diet-Induced Obesity. Microorganisms 9:238.

914 69. Ju T, Kong JY, Stothard P, Willing BP. 2019. Defining the role of *Parasutterella*, a
915 previously uncharacterized member of the core gut microbiota. ISME J 13:1520–1534.

916 70. Hubbard TD, Murray IA, Nichols RG, Cassel K, Podolsky M, Kuzu G, Tian Y, Smith P,
917 Kennett MJ, Patterson AD, Perdew GH. 2017. Dietary Broccoli Impacts Microbial
918 Community Structure and Attenuates Chemically Induced Colitis in Mice in an Ah receptor

919 dependent manner. J Funct Foods 37:685–698.

920 71. Antonson AM, Evans MV, Galley JD, Chen HJ, Rajasekera TA, Lammers SM, Hale VL,
921 Bailey MT, Gur TL. 2020. Unique maternal immune and functional microbial profiles
922 during prenatal stress. Sci Rep 10:20288.

923 72. Huarte-Mendicoa JC, Astiasarán I, Bello J. 1997. Nitrate and nitrite levels in fresh and
924 frozen broccoli. Effect of freezing and cooking. Food Chem 58:39–42.

925 73. Araki Y, Mukaisho K, Sugihara H, Fujiyama Y, Hattori T. 2010. *Proteus mirabilis* sp.
926 intestinal microflora grow in a dextran sulfate sodium-rich environment. Int J Mol Med
927 25:203–208.

928 74. Chang C-S, Liao Y-C, Huang C-T, Lin C-M, Cheung CHY, Ruan J-W, Yu W-H, Tsai Y-T,
929 Lin I-J, Huang C-H, Liou J-S, Chou Y-H, Chien H-J, Chuang H-L, Juan H-F, Huang H-C,
930 Chan H-L, Liao Y-C, Tang S-C, Su Y-W, Tan T-H, Bäumler AJ, Kao C-Y. 2021.
931 Identification of a gut microbiota member that ameliorates DSS-induced colitis in intestinal
932 barrier enhanced Dusp6-deficient mice. Cell Rep 37:110016.

933 75. Khan I, Bai Y, Ullah N, Liu G, Rajoka MSR, Zhang C. 2022. Differential Susceptibility of
934 the Gut Microbiota to DSS Treatment Interferes in the Conserved Microbiome Association
935 in Mouse Models of Colitis and Is Related to the Initial Gut Microbiota Difference.
936 Advanced Gut & Microbiome Research 2022:7813278.

937 76. Gibbons SM. 2020. Keystone taxa indispensable for microbiome recovery. Nature
938 Microbiology 5:1067–1068.

939 77. Duvallet C, Gibbons SM, Gurry T, Irizarry RA, Alm EJ. 2017. Meta-analysis of gut
940 microbiome studies identifies disease-specific and shared responses. Nat Commun 8:1784.

941 78. Walters WA, Xu Z, Knight R. 2014. Meta-analyses of human gut microbes associated with
942 obesity and IBD. FEBS Lett 588:4223–4233.

943 79. Han YW. 2015. *Fusobacterium nucleatum*: a commensal-turned pathogen. Curr Opin
944 Microbiol 23:141–147.

945 80. Gu M, Samuelson DR, de la Rua NM, Charles TP, Taylor CM, Luo M, Siggins RW,
946 Shellito JE, Welsh DA. 2022. Host innate and adaptive immunity shapes the gut microbiota
947 biogeography. Microbiol Immunol 66:330–341.

948 81. Suzuki TA, Nachman MW. 2016. Spatial Heterogeneity of Gut Microbial Composition
949 along the Gastrointestinal Tract in Natural Populations of House Mice. PLoS One
950 11:e0163720.

951 82. Wu S, Zhang B, Liu Y, Suo X, Li H. 2018. Influence of surface topography on bacterial
952 adhesion: A review (Review). Biointerphases 13:060801.

953 83. Stenman LK, Holma R, Forsgård R, Gylling H, Korpela R. 2013. Higher fecal bile acid
954 hydrophobicity is associated with exacerbation of dextran sodium sulfate colitis in mice. J
955 Nutr 143:1691–1697.

956 84. Fahey JW, Smilovitz Burak J, Evans D. 2022. Sprout microbial safety: A reappraisal after a
957 quarter-century. Food Frontiers 1–7.

958 85. Rao M, Afshin A, Singh G, Mozaffarian D. 2013. Do healthier foods and diet patterns cost

959 more than less healthy options? A systematic review and meta-analysis. BMJ Open
960 3:e004277.

961 86. Economic Research Service. Food Access Research Atlas. US Department of Agriculture.
962 https://www.ers.usda.gov/data/fooddesert. Retrieved 22 April 2022.

963 87. Wedick NM, Ma Y, Olendzki BC, Procter-Gray E, Cheng J, Kane KJ, Ockene IS, Pagoto
964 SL, Land TG, Li W. 2015. Access to healthy food stores modifies effect of a dietary
965 intervention. Am J Prev Med 48:309–317.

966 88. Baker EA, Schootman M, Barnidge E, Kelly C. 2006. The role of race and poverty in access
967 to foods that enable individuals to adhere to dietary guidelines. Prev Chronic Dis 3:A76.

968 89. Taghipour N, Molaei M, Mosaffa N, Rostami-Nejad M, Asadzadeh Aghdaei H, Anissian A,
969 Azimzadeh P, Zali MR. 2016. An experimental model of colitis induced by dextran sulfate
970 sodium from acute progresses to chronicity in C57BL/6: correlation between conditions of
971 mice and the environment. Gastroenterol Hepatol Bed Bench 9:45–52.

972 90. Chassaing B, Srinivasan G, Delgado MA, Young AN, Gewirtz AT, Vijay-Kumar M. 2012.
973 Fecal Lipocalin 2, a Sensitive and Broadly Dynamic Non-Invasive Biomarker for Intestinal
974 Inflammation. PLoS One 7:e44328.

975 91. Nocker A, Sossa-Fernandez P, Burr MD, Camper AK. 2007. Use of propidium monoazide
976 for live/dead distinction in microbial ecology. Appl Environ Microbiol 73:5111–5117.

977 92. Pedersen EJ, Miller DL, Simpson GL, Ross N. 2018. Hierarchical generalized additive
978 models: an introduction with mgcv. PeerJ Preprint e27320v1.

979 93. Oksanen J, Guillaume Blanchet F, Friendly M, Kindt R, Legendre P, McGlinn D, Minchin
980 PR, O'Hara RB, Simpson GL, Solymos P, Stevens MHH, Szoecs E, Wagner H. 2020.
981 Vegan: Community Ecology Package (2.5-7). https://cran.r-
982 project.org/web/packages/vegan/vignettes/diversity-vegan.pdf.

983 94. Archer E. 2022. rfpermute: Estimate Permutation p-Values for Random Forest Importance
984 Metrics (2.5.1). https://github.com/EricArcher/rfPermute.

985 95. Wickham H. 2016. ggplot2: Elegant graphics for Data Analysis. Springer Publishing
986 Company, New York. https://dl.acm.org/citation.cfm?id=1795559.

987 96. Kassambara A. 2022. ggpubr:"ggplot2" based publication ready plots (0.1.7).
988 https://rpkgs.datanovia.com/ggpubr/.

989 97. Knights D, Kuczynski J, Charlson ES, Zaneveld J, Mozer MC, Collman RG, Bushman FD,
990 Knight R, Kelley ST. 2011. Bayesian community-wide culture-independent microbial
991 source tracking. Nat Methods 8:761–763.

992 98. Galey M. 2021. Mi-Seq Analysis. GitHub. https://mgaley-004.github.io/MiSeq-
993 Analysis/Tutorials/SourceSink.html, https://github.com/mgaley-004/MiSeq-Analysis.
994 Retrieved 7 December 2022.

995